Design and Analysis of a Stirling Engine Powered by Neglected Waste Heat

Energy and the Environment Bass Connections

Professors: Dr. Emily Klein, Ph.D and Dr. Josiah Knight, Ph.D

Project Team: Chris Orrico, Alejandro Sevilla, Sam Osheroff, Anjali Arora, Kate White, Katie Cobb, Scott Burstein, Edward Lins

26th April 2020

Table of Contents

List of Figures

List of Tables

Acknowledgements

We could not have undertaken this project without the help and support of the Duke University faculty and staff and various industry professionals. We would like to first thank Drs. Josiah Knight and Emily Klein for their guidance and expertise throughout the last year. Without them, this project would not have even been conceptualized or given the resources to be carried out. We would also like to thank Patrick McGuire for his continued work assisting in sourcing parts and for the advice and assistance he provided for the laboratory test setup of our Stirling engine. Likewise, we thank Steven Earp and Gregory Bumpass of the Pratt Student Machine Shop for advising our team on best practice for the manufacturing of our device. Outside of Duke University, we would like to thank Barry Schneider of Steel Dynamics for offering his time and providing inside industry perspective on the feasibility of our technology in the real world. Finally, we want to thank Duke Bass Connections for their continued support for projects like ours.

1 Executive Summary

The design and potential use of a prototype free piston Beta configuration Stirling engine able to produce electricity from low-grade waste heat is explored. The design choices are meant to improve upon existing literature on the efficient construction of similar engines while minimizing the temperature gradient required for the engine to operate. Technical design choices and improvements to previous designs made during this process were based around simplifying manufacturing, assembly, and testing while maximizing engine efficiency. Due to the COVID-19 outbreak, completion of manufacturing became unfeasible, leading to the creation of assembly instructions and speculative process failure modes and effects analyses to be used by a future team working on this engine design project. Following the modelling of the engine, the uses of a scaled 1-kilowatt (kW) version are considered. Guiding our research into the most efficient application of the model are considerations for grade of waste heat, logistics, and feasibility of implementation. Two of the most promising waste heat recovery applications include pairing our model to the steel industry (among other heavy industrial applications) and laundromats. Finally, a life cycle analysis for a scaled 1 kW engine was conducted in order to determine potential CO2 emissions reductions from waste heat recovery as well as social and environmental impacts from manufacture. In this study we recognize both the benefits of and drawbacks of using this technology for our intended range of applications and as a solution to the issue of energy lost as low-grade waste heat.

2 Introduction

A significant challenge in the modern built environment is the capture and utilization of low-grade waste heat. As a fundamental result of thermodynamics, all energetic processes release waste heat. Indeed, of that waste heat, "60% of waste heat losses are at temperatures below 450°F [230°C]."[1] Examples of sources for heat rejection to the environment include: a simple light bulb, running electronics, hot pavement, or exhaust from engines or furnaces. Since this heat often has lower temperatures and lower utility, it is normally just released into the environment. This loss not only decreases system efficiency but can also cause ambient temperatures to rise creating uncomfortable environments for living and working. The 'all-of-the-above' policy approach to decarbonizing an economy requires all angles of renewable energy and energy efficiency to be explored, but how to reduce low grade waste heat (heat less than roughly 450F) is a relatively unexplored area of research.

While some technologies exist to capture and reuse this heat, very few are able to generate electricity directly from the heat source and even fewer can utilize heat at very low temperatures. An example of a mature technology that can do this are thermoelectric generators, though these devices remain inefficient at low temperature gradients. Other technologies, like Organic Rankine Cycles, are far too complex of systems to be cost efficient. A Stirling engine can use a low temperature differential to produce electricity. In addition, it has the added benefit that scaling

---

[1] US Department of Energy

laws have been established to allow the extrapolation of results from a smaller-scale prototype, thus adding value to demonstrating an improved version of an engine on a smaller scale. Motivated by a desire to solve the waste heat issue and develop a relatively low cost, high efficiency, and simple system for producing electricity from low grade waste heat, we explore the feasibility of using a novel Stirling engine design to do just that.

3 Technical Design

3.1 Configuration Selection

The free piston Beta Stirling engine configuration was settled on for several reasons. Among the three main types of Stirling engines (see. Fig. 1 below), the Beta engine represents a linear and compact version that allows the manufacture of the engine as a simple cylindrical pressure vessel. This further reduces manufacturing costs and ease of use. The free piston Stirling engine (FPSE) is a subset of the Beta engine (see Fig. 2), that instead of having the components connected to a crankshaft relies on the use of springs and damping coefficients to control the dynamics. More importantly, the use of a free piston removes the need to overcome the inertia and friction of mechanical connections associated with the crankshaft. In theory, this should increase the engine efficiency and lower the threshold temperature gradient required to produce engine motion.

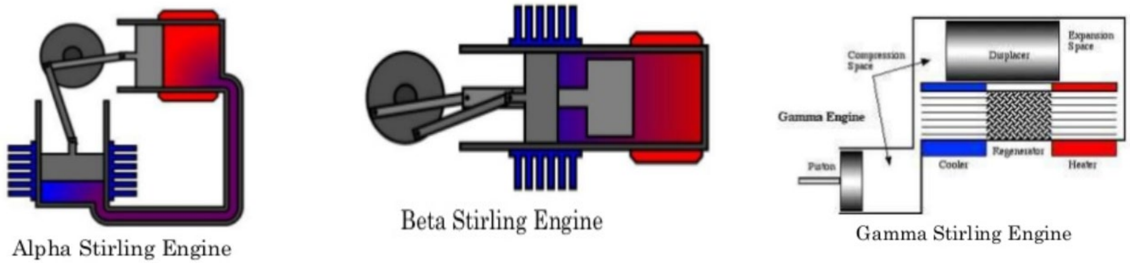

Figure 1: Three main configurations of Stirling engines. Our prototype is a subset of the Beta (center) configuration.[2]

---

[2] Patel, V.

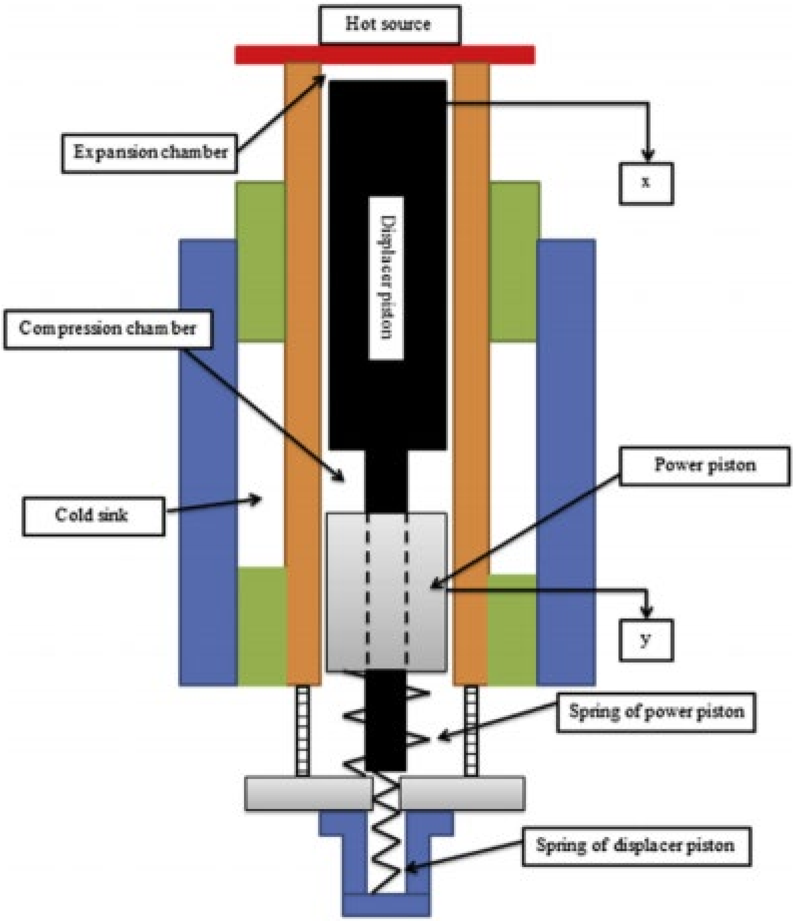

Figure 2: Typical schematic of a FPSE found in literature.[3]

3.1.1 Summary of Design Approach

The approach to designing this engine was intended to build off of existing literature regarding the construction and testing of low-temperature differential FPSEs. After choosing to go with a FPSE design, we used online resources and Dr. Josiah Knight's assistance to develop a model in MATLAB that accounts for dynamic and thermodynamic considerations (see Appendix A for script). This model allows us to predict the motion of the engine components as well as its expected mechanical power output. The process described was an iterative one, in which the parameters fed into the MATLAB model were continuously changed during the physical engine ideation process until a desirable simulation with a proper Stirling cycle and phase shift were achieved. Driving the physical engine design were three main principles: ease of construction/assembly, ease of testing, and safety.

---

[3] Zare, S et al.

3.1.2 Theory

A Stirling engine is a type of heat engine that converts thermal energy into mechanical energy. A heat source provides thermal energy to the working fluid (usually a gas), which then undergoes a series of ideally reversible expansion and compression processes known as the Stirling cycle as the gas heats and cools. Dynamically, the processes are completed with the help of a displacer, which is able to move the gas to the chambers in which the heating/cooling occurs. To be able to extract mechanical power, a power piston seals the gas/displacer space. Due to the pressure variations in this space due to the gas heating/cooling, the piston experiences a net force. The springs attached to the displacer and piston provide a restorative force that allows the motions to occur cyclically, as long as there is a heat source. The net force experienced by the piston can be used to drive a magnet attached to it through loops of wire. This magnetic motion induces current in the wire known as electricity.

3.1.2.1 Thermodynamic Principle

The ideal Stirling cycle is shown below in Fig. 3. In step 1→ 2, isothermal compression of the gas occurs at cold temperature T_c. Then, from 2→ 3, the gas heats at a constant volume as it absorbs heat from the heat source. From 3→ 4, isothermal expansion of the gas occurs at hot temperature T_h. Lastly, during 4→ 1 the gas cools at a constant volume as it transfers heat to its surroundings. During this process, the presence of a regenerator would allow some of the heat rejected during 4→ 1 to be used during the heating 2→ 3 process, thus lowering the amount of heat energy wasted. The net-result of this cycle is mechanical work/energy the pressure-volume changes of the gas induce on the moving engine parts.[4] For a Stirling engine oscillating at frequency f with hot volume V_h,cold volume V_c, regenerator volume V_r and temperature T_r the power output *P* can be calculated using Equation 1 below. *M* and *R* represent the mass and gas constant values, respectively, for the working gas inside the chamber.

$$P = f * \int MR \left(\frac{V_h}{T_h} + \frac{V_c}{T_c} + \frac{V_r}{T_r}\right)^{-1} dV \qquad \text{Eq (1)}^{5}$$

---

[4] Moran

[5] Riofrio, J.A et al.

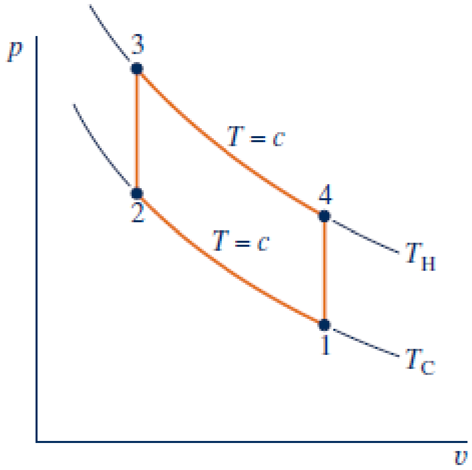

Figure 3: Ideal Stirling Cycle Pressure-Volume (P-V) diagram.[6]

3.1.2.2 Dynamic Principle

In a typical FPSE, the Stirling cycle is completed through the use of several key components: a displacer, a piston, and springs (see Fig. 2 above). The gas is able to move between the hot side (expansion chamber) and cool side (compression chamber) due to the displacer which moves the gas through the space between the cylinder wall and the displacer. As the displacer oscillates with the help of a spring, it is able to affect the pressure of the gas in the working chamber (expansion and compression spaces combined). When the displacer allows gas into the expansion chamber, these molecules gain energy from the heat source and the working pressure increases. The opposite occurs when the displacer moves the gas to the compression chamber, lowering the working pressure as the gas cools. The power piston experiences significant force amplitudes as a result of pressure fluctuations from which it is able to extract useful mechanical work. It is worth noting in the configuration shown, the displacer moves because it is dynamically linked to the piston as well as because it has a small rod extending all the way down to the bounce space to attach its spring and thus exhibits a much smaller force similar to the one described for the piston due to the pressure difference[7].

3.1.2.3 Electromagnetic Principle and Damping

In order to extract electrical power from the mechanical power of a FPSE, a magnet is usually attached to the power piston. The oscillating magnet produces a changing magnetic field through its range of motion. This changing magnetic field can induce a current in conductive material, per Lenz’s law. A linear generator most commonly consists of a magnet (or set of magnets) oscillating

---

[6] Moran. Figure 9.21

[7] Riofrio, J.A et al.

through loops of a conductive copper wire, thus inducing a current in the wire which can be connected to an external load for use.[8]

These currents, known as eddy currents, can create a physical drag force which would oppose the motion of the changing magnetic field in a matter that is proportional to the velocity of the moving magnet. A formula for the damping coefficient as a function of magnet and conductor parameters has been proposed by a few papers.[9] This formula was used to estimate the approximate value of a piston damping coefficient that can be expected by the magnets we could source. Admittedly, the result is not exact but has the advantage that we can adjust said value by adjusting the number of active coils in the generator, thus allowing for flexibility to reach the range of damping we design for.

Similarly, damping was estimated for the displacer due to viscous effects of the gas moving through the regenerative space using an equation found in literature as a function of fluid properties and drag coefficient from its velocity.[10] Nonetheless, similar to the piston damping coefficient, this is simply an estimate that can be experimentally varied with the amount of regenerative material used. While we recognize the lack of robustness in this aspect of the modelling, these estimates were used when validating the MATLAB model with an online paper, who also did not report damping coefficients, as explained later when describing the model.

3.1.3 General Engine Ideation

Literature available on constructed or just simulated FPSEs provide varying degrees of dynamical information, and little to none on construction details. One paper was found to provide the most physical parameters with a size and heat source that were deemed plausible for construction and testing with our available resources. This study allowed us to validate our modelling, as mentioned below. More importantly, our prototype proposes significant changes that we believe would result in a much higher mechanical power output than the one presented (approx. 3 W).[11]

First, our main diameter is much bigger (3.5’’ compared to 1.4’’), this would allow for a higher volume of swept gas thus increasing power output, per eq. 1. Second, we propose using helium as working gas (as opposed to air). Switching to helium would mean the working gas is physically lighter and has a higher thermal conductivity.[12] These properties would presumably allow the gas to move with less difficulty and allow the transfer of heat with greater ease throughout the cycle. Third, we propose the use of regenerative material to increase the efficiency of the cycle, thus resulting in higher power output for the same heat source. Lastly, while their engine configuration (Fig. 3 above) has an extended rod that goes through the piston that could result in some leakage from the working chamber, our engine does not, presumably allowing for less leakage. With these changes in configuration, our MATLAB model was used to find adequate lengths and springs

---

[8] Ebrahimi, B. et al.

[9] Ebrahimi, B. et al; Partha, P. et al

[10] Khripach, N. et al.

[11] Zare, S et al.

[12] Thermal Conductivity

(Appendix A). Having selected engine dimensions, a prototype was designed and modelled in SolidWorks. Design decisions will be further discussed in the Engine Design Prototype section.

3.2 Analysis and Computational Modelling

3.2.1 Dynamic & Thermodynamic Model: MATLAB

Several papers have modelled the dynamics and thermodynamics of a Stirling engine using numerical simulation procedures.[13] Whereas the approaches to solving their models differ, their assumptions and equations of motion (EOMs) were similar and were also used in this study. It is worth noting that "solving" the models in literature consisted in both simulating the motion of the engine components and optimizing their parameters; the MATLAB model presented is limited to simulation and no optimization was performed (Appendix A). The MATLAB model works inside a loop that is set up using the EOMs and critical engine parameters and components. A small force perturbs the piston which sets the engine in motion. The engine's slight motion is then used to calculate an instantaneous working pressure of the gas as a function of instantaneous volumes and constant temperatures; these pressure changes are used to calculate a new force that perturbs the engine. The loop runs until the calculated force is no longer changing and the engine runs at steady state. An ideal result would mean a recognizable pressure-volume graph as well as a phase shift between the piston and displacer as close as possible to 90°, though many papers report working engines with phase shifts with as much as about 30° from this target in either direction.[14]

The most important assumptions for the adiabatic thermodynamic models are:

1. The pressure at any given time in the working chamber is the same.
2. The expansion and compression chambers have constant temperature T_h and T_c, respectively, along with a logarithmic mean difference temperature in the regenerator space T_r.
3. The working gas is an ideal gas.[15] Following the physical engine ideation and consulting with literature and Dr. Knight, the EOMs for our engine are presented below in Fig 4.

The MATLAB model was validated using parameters provided by a published paper, yielding similar amplitudes and phase shift as the ones presented in their work.[16] Understanding frequency would most likely be associated with the heat source and this work had a design frequency of 10 Hz for a 200K temperature difference, a frequency of 10 Hz and 200K temperature difference was kept for our design.

---

[13] Zare, S et al; Riofrio, J et al; Karabulut, H; Sowale, A.

[14] Zare, S et al; Riofrio, J et al; Karabulut, H; Sowale, A.

[15] Karabulut, H.

[16] Zare, S. et al.

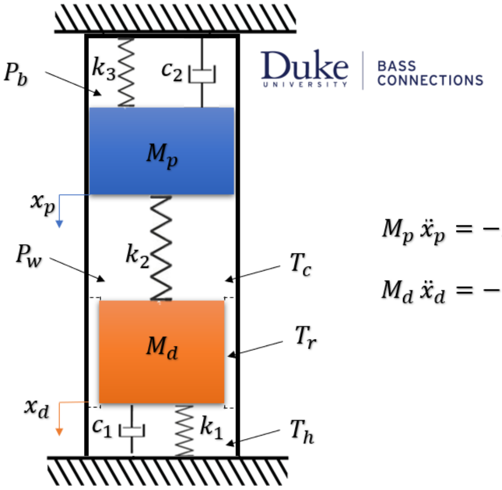

$$M_p \ddot{x}_p = -k_3 x_p - k_2 (x_p - x_d) - c_2 \dot{x}_p + F_{(P_w,P_b)}$$

$$M_d \ddot{x}_d = -k_1 x_d - k_2 (x_d - x_p) - c_1 \dot{x}_d$$

Figure 4: Dynamic Diagram & EOMs for our FPSE prototype.

The following table (Tab.1) summarizes the more critical parameters to our engine model. A more comprehensive list can be found in Appendix E.1.

Table 1: Summary of input parameters to MATLAB model

Parameter	**Value**
Frequency (*f*)	10 Hz
Main diameter (d)	7.62 cm (3.5”)
Hot temperature (T_h)	500K (227℃)
Cold temperature (T_c)	300K (27℃)
Gas & bounce pressure (P_b)	Helium (1.01 bar)

3.2.2 Motion Analysis: SolidWorks

After modelling the individual components of the prototype in SolidWorks, we proceeded to conduct a motion analysis study that considers the same variable inputs and intermediate outputs as the MATLAB model (springs, damping, resulting force). The results can be shown below in Fig 5.

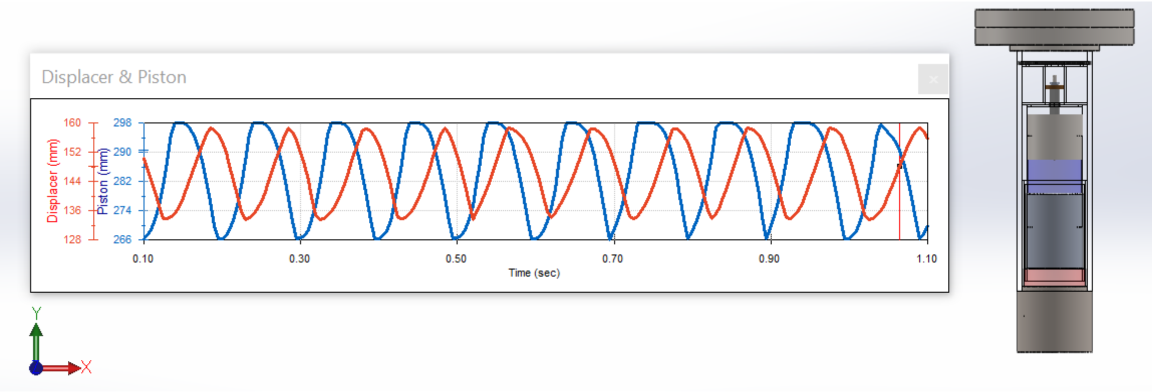

Figure 5: Displacer & Piston Displacement Results from SolidWorks Motion Analysis

A comparison of our MATLAB & SolidWorks Motion Analysis results is summarized in Tab. 2 below. Most notably, while the piston and displacer amplitudes are similar, the phase shifts are distinct, resulting in significant disparity in power output between the two models. The SolidWorks model results in a higher phase shift than the MATLAB one, further away from the 90 degrees ideal target. In turn, this presumably leads to the model's lower predicted power output. While the exact reason for the difference in model phase differences is not known, the group theorized that there could be some frequency-dependent effects (vibrations) in the SolidWorks motion that were not accounted for in the MATLAB model. The pressure-volume diagrams can be seen in Fig. 6 below, as well. It is worth noting none of the models consider fluid viscosity in their calculations, which certainly would have an effect in the actual experimental testing of the engine.

Table 2: Summary of results from MATLAB & SolidWorks models for a 200K temperature difference between the hot and cold volumes

Parameter	*MATLAB Model*	*SolidWorks Model*
Piston Amplitude	1.62 cm	1.61 cm
Displacer Amplitude	1.25 cm	1.22 cm
Phase Shift	85°	108°
Mechanical Power	31 W	23 W

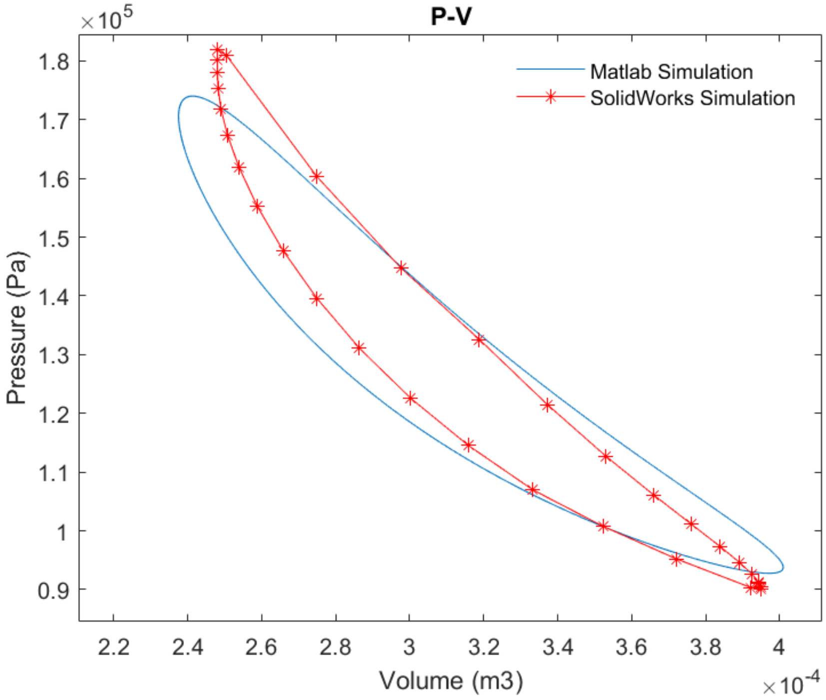

Figure 6: Pressure-Volume (P-V) modelling comparison

3.2.3 Static Spring-Mass System Linear Geometry Calculation

Given an arbitrary cylinder length (defined as 12 inches), two static scenarios were constructed in order to predict and verify piston and displacer linear motion and the resulting engine cylinder geometry. With equations constructed from each scenario, we can construct a relationship between the force of gravity and the extension of each spring to verify that springs of equal spring constants to those determined by the MATLAB modelling process. This relationship will do the following:

1. Ensure that each spring will always be in tension
2. Determine how much of each spring (lengths defined by the offering available on McMaster Carr) must be recessed within abutting surfaces in order to maintain the dead space volumes specified by the MATLAB model.

Each of these parameters represent critical to function geometries. For both scenarios, spring 1 anchors the piston to the top of the cylinder, spring 2 connects the piston to the displacer, and spring 3 anchors the bottom of the displacer to the bottom of the cylinder. The variables are labelled as follows

F_{s1} = Force of spring 1
F_{s2} = Force of spring 2
F_{s3} = Force of spring 3
k_1 = Spring constant 1
k_2 = Spring constant 2
k_3 = Spring constant 3

l_{r1} = Relaxed length of spring 1
l_{r2} = Relaxed length of spring 2
l_{r3} = Relaxed length of spring 3
δ_1 = Initial extension of spring 1 without gravity
δ_2 = Initial extension of spring 2 without gravity
δ_3 = Initial extension of spring 3 without gravity
F_{s1} = Hooke's law tensile force of spring 1
F_{s2} = Hooke's law tensile force of spring 2
F_{s3} = Hooke's law tensile force of spring 3
x_1 = Piston displacement when gravity introduced
x_2 = Displacer displacement when gravity introduced
A_p = Piston Amplitude (from Matlab model)
A_d = Displacer Amplitude (from Matlab model)
m_p = Piston mass
m_d = Displacer mass
g = The gravitational constant
l_{rec2} = The spring 2 recess length required to facilitate a 12-inch cylinder
l_{rec3} = The spring 3 recess length required to facilitate a 12-inch cylinder
l_p = piston length
l_d = displacer length
L = overall length 12 inches

Scenario 1: Extended Without Gravity

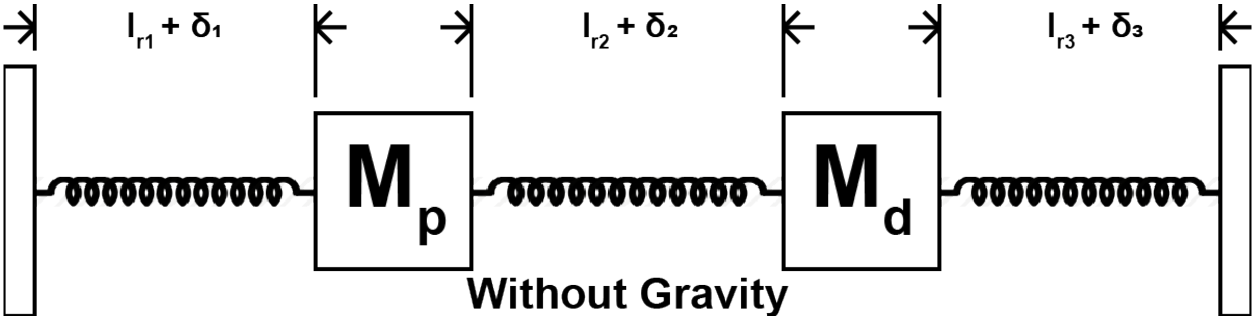

Figure 7: Extended without Gravity

From the sketch above, we attain the following relationships…

$$F_{s1} = F_{s2} = F_{s3} \quad \text{Eq (2)}$$

$$F_{s1} = k_1\delta_1\ (etc), \therefore\ k_1\delta_1 = k_2\delta_2 = k_3\delta_3 \quad \text{Eq (3)}$$

$$L = l_{r1} + \delta_1 + l_{r2} + \delta_2 + l_{r3} + \delta_3 + l_p + l_d \quad \text{Eq (4)}$$

Scenario 2: Extension with gravity

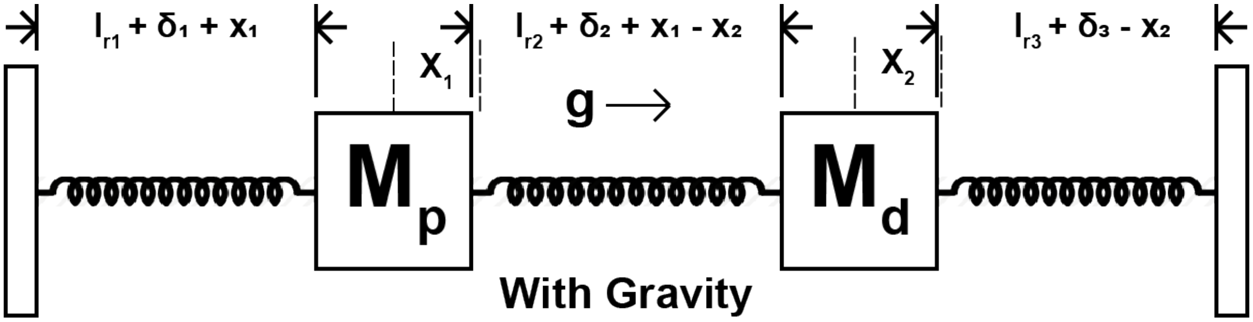

Figure 8: Extended with Gravity

From scenario 2, we attain the following relationships…

$$F_{s1} = F_{s2} + m_p g \quad \text{Eq (5)}$$

$$k_1(x_1 + \delta_1) = k_2(\delta_2 + x_2 - x_1) + m_p g \quad \text{Eq (6)}$$

$$F_{s2} = F_{s3} + m_d g \quad \text{Eq (7)}$$

$$k_2(\delta_2 + x_2 - x_1) = k_3(\delta_3 - x_2) + m_d g \quad \text{Eq (8)}$$

The equations from scenario 1 allow us to determine each value of δ_i for a given overall length, piston length, displacer length, relaxed spring constants, and set of spring constants. The equations from scenario 2 allow us to determine the displacement of the piston and displacer under the influence of gravity. With this system of equations, we can verify the following 'critical to function' (CTF) relationships:

$$(\delta_2 + x_2 - x_1) > A_p + A_d \quad \text{Eq (9)}$$

$$(\delta_1 + x_1) > \ A_p$$

$$(\delta_3 - x_2) > \ A_d$$

To reiterate, these relationships are CTF because they determine whether each spring will be in tension at all points within the Stirling cycle. If a spring were to lose tension, it would cause a radial deflection in either the piston or displacers motion and possibly jam the engine. Given that spring selection was limited by availability on McMaster Carr, spring selection was iterative. By this, we mean that a set of springs that were as short and robust as possible were selected based on desired spring constants. Each spring's characteristics were then plugged in to the above equations to verify the CTF criteria were met. This was done in Maple for efficiency. The final iteration and applied code can be found in Appendix B and the final spring values are listed below.

Table 3: Spring values

	Spring constant (N/m)	Spring Relaxed Length (Inches)
Spring 1	1388	2.75”
Spring 2	485	3”
Spring 3	275.3	2”

Finally, recessed lengths were calculated from the overall length compared to scenario 2. Recessed lengths are likewise CTF as they maintain the required dead space above the displacer and between the displacer and piston. The calculations are as follows…

$$l_{rec2} = (l_{r2} + \delta_2 + x_2 - x_1) - 4cm\ (static\ distance\ between\ piston\ and\ displacer) \quad \text{Eq (10)}$$

$$l_{rec3} = (l_{r3} + \delta_3 - x_2) - 3cm\ (static\ distance\ between\ displacer\ and\ bottom) \quad \text{Eq (11)}$$

Table 4: CTF Relationships

Relationship	Value	Value to Exceed for CTF
$\delta_2 + x_2 - x_1$	3.21cm	2.87cm
$\delta_1 + x_1$	2.67cm	1.62cm
$\delta_3 - x_2$	4.96cm	1.25cm
l_{rec2}	7.41cm	-
l_{rec3}	7.04cm	-

From these CTF values, the length of the piston, the length of the displacer, the neutral distance between the displacer and piston, the magnet assembly length, overall cylinder length and end cap countersink lengths can be calculated. Any alterations to the above spring values required recalculating the above values and the cylinder dimensions. Should a future team attempt to modify the overall engine design, we recommend purchasing custom springs that are short enough to drastically reduce the recess lengths (such springs are unavailable off of the shelf).

3.2.4 FEA & Thermal Studies

An FEA study on the pressure vessel looked into yielding due to the internal pressures we anticipate reaching (≤ 2 bar). This resulted in a max stress of 133 psi, with safety factor n>240 for our thick-walled steel pressure vessel (see Appendix C). While this is not a failure we anticipate, other possible modes of failure are considered. Principally, we anticipate interfacial pressure leaks due to poor pipe connections. This would occur either as a slow leak at the pipe fittings for the connections between the piston cylinder and bounce space, or as a pressure leak around the wire strain relief fittings could occur. Despite the high rating of the Teflon tape being used to seal the threads, this could occur due to testing as the engine will have to be assembled and disassembled several times. A secondary mode of failure along these lines could occur as a failure in the gasket that creates a face seal between the cap flange that closes the top of the piston cylinder.

A thermal study was conducted to determine whether external experimental cooling would be needed. With a heat source providing an approximate 200℃ temperature in the hot chamber, the cold chamber will get as hot as ~90℃ (see Appendix C) It is in our best interest to lower the temperature of the cold chamber to room temperature (~23℃) to achieve a higher temperature differential, which we hope to experimentally achieve with the use of cooling water, as explained later.

3.3 Engine Design Prototype

Aside from fundamental geometry, masses, and spring parameters, decisions for the practical design of the engine were guided by three major considerations:

1. Machinability
2. Ease of assembly and disassembly
3. Safety

Regarding manufacturability, it was our goal to minimize the number of machining operations and maximize the number of stock parts that could be readily purchased. There were multiple motivations for this. First, we sought to make the engine as simple as possible for students to manufacture with the resources available in the Pratt student machine shop. Second, sourcing stock parts and reducing machining operations ensured that costs involved in prototype manufacturing are also minimized. It should be noted that the cost per watt of power produced will be relatively high for this prototype.

With testing planned as an important component of the experimental engine design, it was necessary to design an engine that could be readily assembled and disassembled to modify or replace parts as needed. This motivated the design of a stationary but removable stack of components within the engine cylinder, consisting of the Regenerator Housing, Sleeve Bearing, and Generator Housing. The component stack is held in place by a removable snap ring. Threaded connections were included between the masses (displacer and power piston) and the springs in order to allow changing out of springs should it become necessary. A further design modification was made by adding a threaded plug to the end cap to make insertion of the displacer and piston easier. By removing all but essential permanent connections (essential connections such as weldments), a level of variability was afforded to maximize the likelihood of engine success.

Finally, a strong consideration was safety. Even pressurizing the engine to a mean pressure of 2 bar presents a considerable risk to those testing the engine under these conditions. As such, the engine's outer shell was designed as a thick wall pressure vessel (Appendix C). As referenced in the previous section, the pipe wall that was selected was as thick as possible to maximize the factor of safety. SolidWorks CAD files of the complete engine design will be supplied with this report (Appendix D).

3.4 Manufacturing

This section will discuss part machining and engine assembly. Due to the COVID-19 outbreak beginning in March of 2020, completion of engine construction was not feasible within the initially proposed design timeline. Instead, we provide a comprehensive guide and suggest solutions for anticipated complications such that an independent research group or contractor could construct our proposed engine design.

It should be noted that this section has mutually reinforcing sections. The user ought to first review the assembly procedure, which itself will reference the technical drawings and machining instructions in Appendix E. Before beginning assembly, the user also ought to consult the speculative process failure mode and effects analysis (PFMEA) sections and familiarize themselves with possible issues that may arise during manufacturing and proposed solutions for how to overcome those issues (Appendix F).

3.4.1 Assembly Procedure

To begin, the user ought to consult the proposed bill of materials provided in Appendix G. This is a comprehensive bill of materials for both the manufacturing and testing of the Stirling engine prototype. This bill of materials includes cost calculations for materials in the case that (a) the designers have access to the Duke University Mechanical Engineering labs and (b) all parts must be purchased outright. The assembly procedure, provided in Appendix H, will walk the user step by step through the process of machining and assembling the engine. The assembly procedure will reference the technical drawings for specific instructions on machining individual parts. It also references entries in the PFMEA as relevant. The designers of this engine anticipate that the following machines will be necessary to assemble the engine prototype:

- CNC Lathe
- CNC Mill
- 3D Printing with the capability to print steel. Our quotes were through Duke Bluesmith using 17 4 PH stainless steel printed on a Desktop Metal Studio System™ printer.
- Basic FDM 3D printer (we recommend the Ultimaker S3)

3.4.2 Technical Drawings

Technical Drawings of the Stirling engine, including the…

- Overall engine model
- Machining instructions for individual parts
- Welding diagrams

...Are provided in Appendix E. These should be referenced as specified by the assembly procedure in Appendix H.

3.4.3 Process Failure Mode and Effects Analysis

In order to preempt possible complications involved with engine manufacturing, testing, and operation, a process failure mode and effects analysis (PFMEA) was conducted by the designers of this engine. It should be noted that this PFMEA was not conducted through observation of an existing manufacturing process. Due to the inability to manufacture this engine, the PFMEA is entirely speculative. As such, the standard qualitative measures of severity, occurrence, and detection are likewise speculative. All possible modes of failure must be considered and changes to the design must be made as failure modes occur. We therefore propose solutions to each of these modes of failure in order to provide a response to any issues an independent group may encounter when construction of this engine. The PFMEA for manufacturing, testing, and operation can be found in Appendix F.

3.5 Testing, Evaluation and Results

3.5.1 Test Setup

To test the functionality of the Stirling engine prototype, an experimental setup was conceptualized and planned for implementation to supply the temperature differential, path for power output, and pressure required to generate measurable power output from the engine. This experimental setup includes the following sub-assemblies, listed here with a brief description of their working principles and justifications. A full list of the components required for testing can be found in the bill of materials in Appendix G, while assembly instructions for the experimental setup may be found in Appendix I.

3.5.1.1 Test Shield

The test shield is constructed from an 80-20 10-series erector frame and ⅛” thick acrylic sheeting. Dimensions of the area protected by the full test shield assembly are as follows: 12.5” x 12.5” x 21.5”. The thickness of this sheeting was chosen so as to provide ample protection from impact forces due to potential pressure fitting or engine body failure. A hinged door in the sheeting serves to allow tubing and wiring to pass from the shield interior, which houses the engine. The bottom of the shield is kept free of sheeting so as to allow for the shield to be placed over top of the engine. A 4” overhang of 80-20 frame on the bottom of the shield allows for the base to be weighed down with exterior weights so as to minimize frame movement during testing.

3.5.1.2 Cooling coil

The cooling coil is designed to lower the temperature of the cold side area of the experimental engine as close to 23°C as possible, such that the temperature differential between hot and cold sides is large enough for the engine to run. As described in the prior section on FEA and thermal studies, this engine run without a cooling element would see a temperature of as high as 90°C on the cold side due to conduction of heat added to the warm side.

Such cooling is attained utilizing convective and conductive heat transfer, in a process with a similar working principle to a basic heat exchanger. A SEAFLO 21-series diaphragm pump is run to pump cold tap water at 1.2 gm from a reservoir through a ¼” OD copper coil wrapped around the cold side of the engine. Setup of the cooling coil assembly is detailed in Appendix I.

It is possible that this first basic cooling coil may not lower the cold side temperature close enough to 23°C to enable the engine to generate power, a failure condition described further in the “Testing” section of the PFMEA in Appendix F. Should this condition occur, a number of remedies may increase the convective heat transfer an appreciable amount, including adding coolant to the reservoir and purchasing a more expensive pump with a higher flow rate. With the materials at hand, however, the basic cooling coil described previously was determined to be an acceptable first attempt at attaining the desired cold side temperature.

3.5.1.3 Heating coil

The heating coil was chosen to supply the engine with a hot side temperature of 200°C, a value safely consistent with the lower level waste heats analyzed for engine applications. A 400 W Tempco band heater was chosen so as to allow for increases in hot side heat flux up to and above the flux required for a 200°C hot side temperature, should the 200°C value prove either more difficult to attain or not high enough to generate the desired power output. Heat flux calculations are included in Appendix J, while control instrumentation of the heating coil is described in the following section.

3.5.1.4 Instrumentation and measurement

1. Power output

   The working principle of the experimental engine’s power generation, as described in a previous section on “Electromagnetic Principle and Damping” involves linear motion of a magnet attached to the piston inducing current in a coiled linear generator wire. Calculations in Appendix J estimate 1312 wire turns (11m of coil) are possible around the area through which the magnet moves, an axial path of twice the estimated piston motion amplitude. To measure power output, the ends of this coil will be connected to a load resistor, and voltage across the resistor will be measured and recorded via a DAQ board and a LabVIEW VI. As identified in the calculation section, a load resistance equal to the estimated coil resistance of .5 Ω will yield the maximum power transfer. With practical material limitations, such a resistance is most easily attained by wiring two 1Ω resistors in parallel.

2. Heating coil control

   To reach and maintain a hot side temperature of 200°C, a closed control loop connecting a temperature reading to heating coil power supply is required. The hot side of the generator will be instrumented with a thermocouple, which will feed into a data input pin of a data acquisition (DAQ) board. The power output to the heating coil will be controlled by a DAQ output connected to a relay. In this way, source power will be supplied to the heating coil via pulse width modulation (PWM) implemented with a LabVIEW VI. A PID control loop in LabVIEW will serve to relate the power output to the temperature reading, allowing the temperature to be maintained at 200°C. Tuning of this control loop prior to experimental testing will be required to ensure that the system properly attains and maintains the target temperature without excessive overshoot or variation.

3. Other data

In addition to the data values for hot side temperature and load resistor voltage drop, data will also be collected for the cold side temperature to measure the effectiveness of the convective cooling system.

A comprehensive analysis of the failure modes of the experimental setup may be found in the test setup subsection of the PFMEA in Appendix F.

Of importance to the general safety of experimenters is both the use of personal protective equipment (PPE) and a knowledge of the potentially dangerous planes, areas, and components of the control setup. Experimenters are advised to wear protective eyewear at all times, and exercise caution when handling wired components and the heating coil to minimize risk. Dangerous planes include the area directly outside the window in the test shield through which the wires and tubing are passed, as well as the paths along which pressure fittings in the engine body would be most likely to eject. Experimenters are advised to avoid being present in these areas during engine operation whenever possible.

3.5.2 Testing Approach

As the function of the engine will not yet be confirmed at the time of first experimental implementation, a series of tests before operation at full pressure with helium gas is recommended for the purposes of both safety and ease of troubleshooting. Testing should be conducted in the following sequence:

Table 5: Testing Iterations

Test Iteration	**Working Fluid**	**Pressure**
1	Air	Atmospheric
2	Air	2 bar
3	Helium	Atmospheric
4	Helium	2 bar

A speculative set of instructions for experimental procedure may be found in Appendix K. Based on analysis of the potential engine failure modes, test iteration 1 would be the step of the experiment at which the majority of compromising failures would be expected to occur. Should the engine begin moving and generate an amount of power within a reasonable range of the expected values for this stage, continuation to further iterations of testing should yield useful experimental results as to the effects of temperature and working fluid on engine functionality. Alternatively, should the engine not demonstrate proper functionality during test iteration 1, both the assembly and use case sections of the failure mode analysis in Appendix F should be referenced to determine possible causes of engine failure.

3.5.3 Expected Results

Using the geometries and material properties of the chosen Stirling engine setup, hand calculations were performed to determine expected power output values during experimentation. These calculations are included First, the number of wire turns were calculated using the geometry of the linear regenerator slot, as well as the accompanying coil resistance of this length of wire: 1312 turns, resulting in a coil resistance of 0.5823 Ω (Appendix J). Next, two methods were used to calculate magnetic flux, such that values for emf were derived. The following equations relating flux, magnetic flux density, and coil area were used:

$$d\Phi_b = \int B_r exp(-r/\delta) dr d\theta \qquad \text{Eq (12)}$$

$$d\Phi_b = B_r * A \qquad \text{Eq (13)}$$

Where B_r is taken from magnet specifications (1.37T), r describes the distance of the coil from the center of the magnet, θ represents the angle and coil turns, and δ denotes magnetic skin depth of copper. The following equation was used to then calculate the electromagnetic force associated with magnet motion:

$$emf = N * d\Phi_b * f \qquad \text{Eq (14)}$$

which led to values of 5V and 8V from the above two magnetic fluxes, respectively. Based on previous Stirling engine literature, the 5V emf value was chosen[17]. Finally, Ampere's law and the equation for power were used to calculate expected current and associated power power output[18]:

$$P_{out} = emf * I - I^2 * R_{coil} \qquad \text{Eq (15)}$$

$$H * l_m = N * I \qquad \text{Eq (16)}$$

Where I represents current, R_{coil} represents the above calculated coil resistance, H represents field strength as calculated by H=B/N, and l_m represents mean coil turn length. These calculations led to a final expected output power of 1.87 W. While experimentation will be required to confirm the fidelity of this value to the functioning experimental setup, an expected output value of 1.87 W may serve as the first step towards determining that the setup is working properly with a single magnet.

---

[17] Susana et al.

[18] Eriksson

3.6 Scaling

3.6.1 Power Output

This prototype was designed to generate a proof of concept that could then be scaled to produce a larger amount of power. To understand how this model could be scaled, two methods of predicting power output for Stirling methods can be used. These methods are the Beale and West numbers.

The Beale number is used to characterize the performance of a Stirling engine. It is defined as

$$B_n = \frac{W_o}{P_m f V_o} \qquad \text{Eq (17)}$$

Where B_n is the Beale number, W_O is the power output of the engine, P_m is the mean pressure of the engine, f is the engine cycle frequency, and V_O is the volume swept by the piston.

The West number is another way to characterize the performance of a Stirling engine, and uses the Beale number as a part of this calculation, but also considers the temperature dependence of the engine. The West number is calculated by

$$W_n = B_n \frac{T_h + T_c}{T_h - T_c} \qquad \text{Eq (18)}$$

where T_h is the hot temperature and T_c is the cold temperature.[19]

Both of these non-dimensional numbers can be used in order to determine the power output of a larger engine based on the prototype. In order to do this, the power output of the prototype needs to be determined through testing, as discussed in the Discussion, Evaluations, and Results section above. Once this is determined, both the Beale and West numbers can be calculated for the prototype and used to determine how much power the same design would generate with a given piston size.

3.6.2 Beale and West Estimates

Estimates of the Beale and West numbers can be calculated based on the MATLAB and SolidWorks models of the prototype. For the Beale number, the prototype's power output, mean pressure, frequency, and swept volume of the piston must be known. The power output of the prototype, modelled in SolidWorks, was found to be 23 W. It's mean pressure frequency, and swept volume were designed to be 1 bar (or 101325 Pa), 10 Hz, and 1.63×10^{-4} m^3, respectively. Inserting these numbers into the equation for the Beale number (Eq 17) gives that the Beale number for the engine is 0.14.

In order to find the West number, the Beale number and the hot and cold temperatures must be used. The prototype was modelled to be tested with hot and cold temperatures of 500 K and 300

---

[19] Connor Speer et al.

K, respectively. Inserting these numbers into the equation for the West number (Eq 18) gives that the West number for the engine is 0.56.

3.6.3 Manufacturing Cost

In order to determine the manufacturing costs for a 1 kW engine, several factors of the differences between prototype manufacturing and large-scale manufacturing have to be taken into account. Some of these factors include the size of the parts, the methods of part production and assembly, and volume discounts. The increase of part sizes and machining would contribute to an increase in cost, while the volume discounts and automation of production would contribute to a decrease in cost.

3.6.3.1 Increase in Part Size

To determine the increase in cost associated with the increase in size from the prototype engine to a 1 kW engine, the needed increase in part size was determined, and the cost was scaled accordingly.

In order to determine the size of the Stirling engine needed to produce 1 kW, the Beale number calculated based on the prototype, 0.14, can be used. By inserting this Beale number, the desired power output of 1 kW, the mean pressure of 1 bar, and the frequency of 10 Hz into the equation for the Beale number, the corresponding volume that must be swept by the piston in a 1 kW engine can be calculated to be 0.00705 m^3.

The diameter of the volume swept by the piston's prototype is 0.0889 m, and the height is 0.0263 m. These must both be increased to meet the requirement of 0.00705 m^3 swept by the piston for a 1 kW engine. Keeping the ratio of the diameter and height the same, the new diameter is 0.312 m, and the new height becomes 0.0923 m. This means that the diameter and height of the swept volume of the piston increased by about 3.5 times. Although the swept volume of the piston is an indicator of the total increase in size of the engine, many of the other parts would scale at a lesser rate. Therefore, the overall increase in size of the engine was estimated to be by about a factor of 3, and the associated cost increase was also estimated to be by about a factor of 3.

3.6.3.2 Volume Discounts

In general, purchasing in bulk usually results in receiving discounts due to volume. Based on previously seen rates, the volume discount was assumed to be between 30 and 50%.[20]

3.6.3.3 Machining Costs

Machining costs for a 1 kW engine were calculated by multiplying the estimated cost of CNC (Computer Numerical Control) machining per hour by the estimated number of hours it would take to machine the engine. The estimated cost of outsourcing CNC (Computer Numerical Control)

---

[20] Knight.

machining was about $70 per hour[21], and the estimated number of hours it would take the machine the engine was about 7 hours. This implied that it would cost about $500.

3.6.3.4 Automation of Production

Automation of production usually results in a decrease in costs, as processes are streamlined and products are manufactured at a much faster rate. This factor was estimated to contribute about a 15% decrease in total cost.[22]

The cost of the prototype (including the commercial costs of items that were obtained for the Duke Mechanical Engineering Laboratory) came to $1364.03. Considering the factors above, the price to produce a 1 kW engine in a scaled production process was estimated to be about $2500.

4 Engine Applications

4.1 Discussion of Target Markets: Reducing Unused Waste Heat

While focusing on the technical details of ensuring the engine will be able to be manufactured and produce electricity, we also considered how the technology can be applied outside of a lab setting. Since the goal of the Stirling engine idea was to make use of unused heat in the built environment, we began to focus on areas and processes with unused waste heat. In the early phases of the Stirling engine's design, we considered seven applications including heat from pavement, heat from roofs and attics, waste heat exhausted from commercial kitchens, heat absorbed by solar panels, waste heat released within data centers, waste heat exhausted by industrial laundromats, and waste heat from industrial manufacturing processes. In order to analyze for which of these applications the engine design would be most effective, we delved deeper into understanding the heat differences (between the heat source and sink), application logistics, and feasibility.

After understanding more about each potential application, we narrowed our focus by employing a decision matrix (Tab. 6) in which all seven applications were assigned a rating on a scale from one to five (five being best) for their performance in five different categories: heat difference, ease of implementation, distribution of heat, utility of output, and consistency of heat. Heat difference was defined to be the difference between the heat source of the application (e.g. the heat absorbed by pavement, the heat exhausted from a stovetop in a kitchen) and the heat sink (e.g. outside air). Ease of implementation was defined as the level of difficulty of setting up the engine in the context of each application. For example, pavement was given a 1 in this category as construction would need to be done to place the engine underneath existing pavement. Distribution of heat was defined as the concentration of heat in the medium surrounding the engine. For example, an application where heat was channeled to the engine using a liquid medium would have a higher score than one where heat was channeled using air. Utility of output was defined as the relative impact and ease of use the electricity generated would have for each

---

[21] Varotsis, Alkaios

[22] "The (Many) Benefits of Outsourcing Your Manufacturing."

application. Consistency of heat was defined as the regularity of the heat source (e.g. how many hours or days a week a laundromat is in operation). The scores for each category were summed, and the four highest scoring applications, industrial steel, laundromats, data centers, and solar panels were given greater consideration.

Table 6: Decision Matrix Comparing Seven Stirling Engine Applications

	Ind. Steel	**Laundro-mats**	**Data Centers**	**Solar PV**	**Pavement**	**Roofs/Attics**	**Kitchens**
Heat Difference	**5**	**2**	**1**	**1**	1	1	2
Ease of Implementation	**3**	**4**	**4**	**3**	1	1	3
Distribution of Heat	**4**	**3**	**4**	**4**	2	2	3
Utility of Output	**1**	**4**	**3**	**4**	3	4	3
Consistency of heat	**4**	**4**	**4**	**3**	3	3	3
Total	**17**	**17**	**16**	**15**	**10**	**11**	**14**

4.1.1.1 Data Centers

Data centers were given consideration due to the large amount of waste heat they produce and their large carbon footprint. Data centers make up approximately 3% of global electricity usage and roughly 2% of global greenhouse gas emissions[23], but 98% of the energy they use becomes low temperature waste heat[24]. Furthermore, the waste heat exhausted by data centers contributes to their large electricity usage, as servers will fail if they overheat, so care must be taken to remove the waste heat being emitted by servers, and thus cooling the servers can comprise roughly 43% of a data center's electricity budget[25]. However, while a large amount of waste heat is exhausted from data centers, the heat itself is very low grade. We had envisioned the hot server exhaust being channeled to the hot side of the Stirling engine, which would be insulated from the cold side of the Stirling engine, which would be exposed to ambient air temperature. For air-cooled servers, the hot air exhaust can reach to between 28 and 35 °C[26], which, compared to an ambient air temperature of 20 °C, is too small a heat differential for our Stirling engine to operate. Liquid cooled servers offered a potential pathway for our engine, as liquid cooling enables the servers to withstand temperatures of around 45 °C[27], but, once again, the heat differential is too small for our Stirling engine to operate. Ultimately, the low heat differential made us decide to pursue other applications. While we decided to move on from this application, research teams interested in

---

[23] Bawden, Tom
[24] Monroe, Mark
[25] Shehabi, Arman, et al.
[26] Monroe, Mark
[27] Iceotope

harvesting waste heat from data centers with Stirling engines may find possible avenues forward with the use of heat pumps, which can be used to increase the temperature differential.

4.1.1.2 Photovoltaics

Photovoltaics was considered as a potential application due to its apparent storage of heat and rapid growth of installations across the U.S. and globally; it is widely viewed as an efficient source of renewable energy. Our hope was that the Stirling engine could be integrated within a solar farm to boost electricity production and reduce the amount of sensible heat lost to the environment. After performing basic cost analyses, we eliminated the notion of mounting Stirling engines on individual solar panels, for this would be far too expensive. This would have mirrored the setup of a photovoltaic thermal (PVT) panel, which is common in Europe but relatively underutilized in North America. With this possibly gone, the next logical configuration would be to install a liquid cooling system that absorbs heat from multiple solar panels in a solar farm, concentrating the heat to be applied to one Stirling engine. Though this particular use of a heat sink would be more economical, the low heat differential (~50˚F)[28] common across commercial solar panels proved inefficient for our Stirling engine, which requires a much higher heat differential to generate a useful amount of electricity.

While we were initially optimistic regarding this application, the reality is that the variables which would increase Stirling engine utility (high panel temperatures, ease of transferring said heat) ultimately decrease the primary efficiency of the solar panels, which means that installing a Stirling engine would be both cost prohibitive and generate less electricity than is necessary for feasible implementation. For these reasons, we stopped considering photovoltaics as a viable application for Stirling engines. Under these considerations, further developments in heat sink efficiency and cost reductions in Stirling engine construction would potentially make photovoltaics a more attractive application.

4.2 Industrial Waste Heat Application Analysis

4.2.1.1 Background

One of the largest sources of energy use and carbon dioxide emissions in the United States is the industrial sector. This sector consumes about 32 quadrillion Btu of energy per year with about 5-13 quadrillion Btu per year of that energy being discarded as waste heat in the form of hot exhaust gases or liquids as well as heat conduction, convection, and radiation from hot surfaces within manufacturing processes.[29] Waste heat losses are inevitable in manufacturing activities, but can be reduced by increasing efficiency or used for more productive means if captured and recovered.

Currently few technologies exist to capture and reuse this waste heat despite the fact that it can be an emission-free substitute for purchased fuels and electricity. Current recovery methods are limited by costs, emission temperature restrictions, emission chemical compositions, equipment

---

[28] Marsh, J.
[29] Johnson, I. et al.

specific constraints, and feasibility constraints. In terms of cost, existing technologies have long payback periods, costly materials, and high maintenance costs. Temperature restrictions exist for processes with low temperature heat that is not viable for existing recovery processes. Additionally, even processes with high temperature heat cause complications to the varying mechanical and chemical properties at high temperatures. In terms of chemical composition restrictions, most of the waste heat exhaust contains abrasive chemicals which can corrode recovery equipment causing environmental, maintenance, and cost concerns. Finally, existing technologies for waste heat recovery are limited in terms of feasibility of implementation due to limited physical space in some facilities, difficulty in accessing and transporting the heat, and equipment specific hindrances.[30] Thus, there is a considerable need for new methods of capturing and recovering waste heat from industrial processes that adequately address the aforementioned challenges.

The industrial sector is quite broad, including a variety of production schemes with varying amounts of energy use and waste heat with varying temperatures. The waste heat can be qualified as high (> 1,200 °F), medium (450-1,200 °F) or low (< 450 °F) temperature. Figure (9) details some examples of waste heat sources and the temperature range in which they belong along with current advantages and disadvantages to recovering that heat.[31]

Some of the largest energy consuming and waste heat emitting manufacturing processes include glass, cement, iron and steel, and aluminum production in addition to metal casting, industrial boilers and ethylene furnaces. The glass industry consumes about 300 TBtu of energy per year.[32] The majority of this energy is used to melt and refine glass in high temperature furnaces which can be regenerative, recuperative, oxyFuel, electric Boost, or direct melter furnaces. The exhaust temperatures vary depending on the type of furnace between about 800 °F and 2,600 °F, with regenerative and electric boost being the lowest and oxyFuel and direct melter being the highest.[33]

The cement industry ingests about 550 TBtu of energy per year. The first steps in cement production include mining and quarrying for the limestone and chalk, crushing and grinding of these raw materials, producing the clinker in the kilns, and then milling the cement.[34] About 90% of the energy input is used in the clinker production which involves passing the raw materials through hot zones within the kilns in order to produce the solid material called clinker. The kilns are typically large refractory-lined steel tubes which exhaust gases at about 840 °F.[35]

---

[30] Johnson, I.et al.
[31] Johnson, I.et al., 8.
[32] Johnson, I.et al., 45
[33] Johnson, I.et al., 35
[34] Johnson, I.et al., 35
[35] Johnson, I.et al., 35

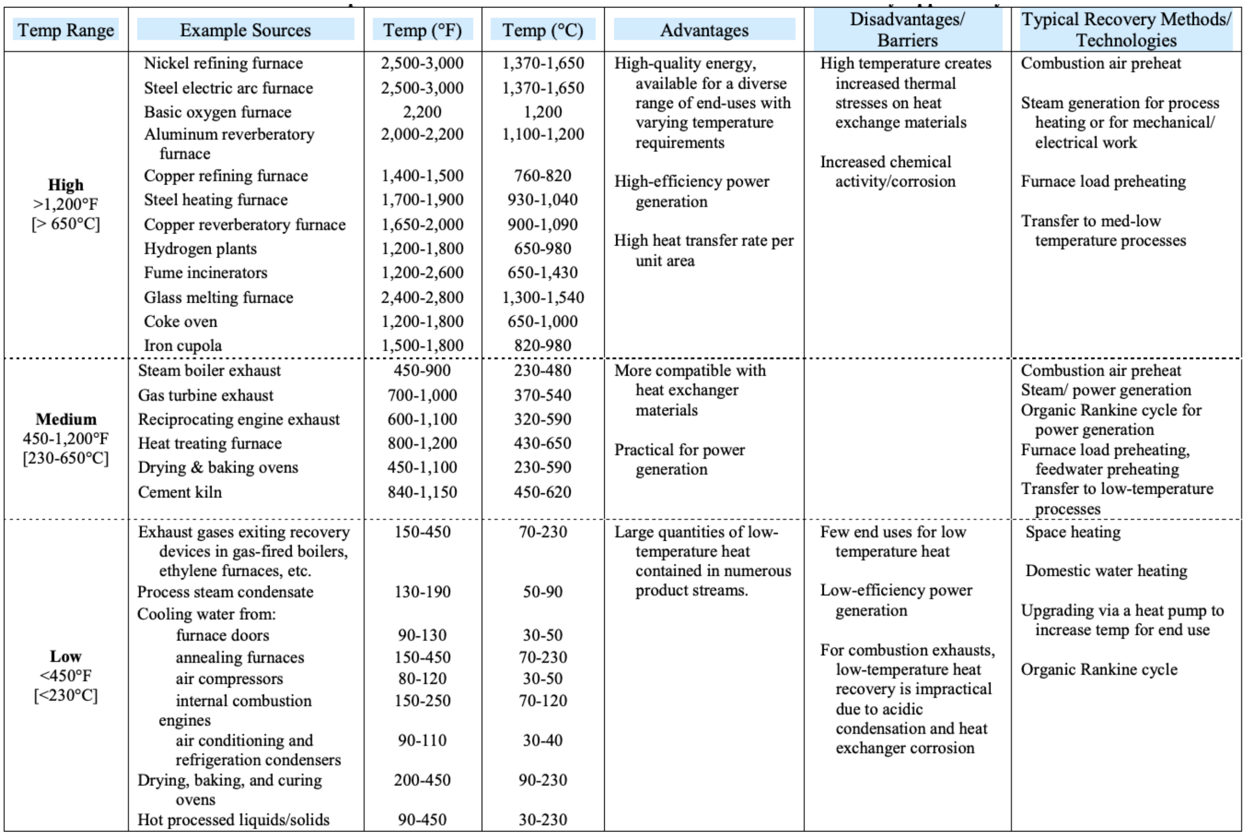

Temp Range	Example Sources	Temp (°F)	Temp (°C)	Advantages	Disadvantages/ Barriers	Typical Recovery Methods/ Technologies
High >1,200°F [> 650°C]	Nickel refining furnace Steel electric arc furnace Basic oxygen furnace Aluminum reverberatory furnace Copper refining furnace Steel heating furnace Copper reverberatory furnace Hydrogen plants Fume incinerators Glass melting furnace Coke oven Iron cupola	2,500-3,000 2,500-3,000 2,200 2,000-2,200 1,400-1,500 1,700-1,900 1,650-2,000 1,200-1,800 1,200-2,600 2,400-2,800 1,200-1,800 1,500-1,800	1,370-1,650 1,370-1,650 1,200 1,100-1,200 760-820 930-1,040 900-1,090 650-980 650-1,430 1,300-1,540 650-1,000 820-980	High-quality energy, available for a diverse range of end-uses with varying temperature requirements High-efficiency power generation High heat transfer rate per unit area	High temperature creates increased thermal stresses on heat exchange materials Increased chemical activity/corrosion	Combustion air preheat Steam generation for process heating or for mechanical/ electrical work Furnace load preheating Transfer to med-low temperature processes
Medium 450-1,200°F [230-650°C]	Steam boiler exhaust Gas turbine exhaust Reciprocating engine exhaust Heat treating furnace Drying & baking ovens Cement kiln	450-900 700-1,000 600-1,100 800-1,200 450-1,100 840-1,150	230-480 370-540 320-590 430-650 230-590 450-620	More compatible with heat exchanger materials Practical for power generation		Combustion air preheat Steam/ power generation Organic Rankine cycle for power generation Furnace load preheating, feedwater preheating Transfer to low-temperature processes
Low <450°F [<230°C]	Exhaust gases exiting recovery devices in gas-fired boilers, ethylene furnaces, etc. Process steam condensate Cooling water from: furnace doors annealing furnaces air compressors internal combustion engines air conditioning and refrigeration condensers Drying, baking, and curing ovens Hot processed liquids/solids	150-450 130-190 90-130 150-450 80-120 150-250 90-110 200-450 90-450	70-230 50-90 30-50 70-230 30-50 70-120 30-40 90-230 30-230	Large quantities of low-temperature heat contained in numerous product streams.	Few end uses for low temperature heat Low-efficiency power generation For combustion exhausts, low-temperature heat recovery is impractical due to acidic condensation and heat exchanger corrosion	Space heating Domestic water heating Upgrading via a heat pump to increase temp for end use Organic Rankine cycle

Figure 9: Different Categories of Waste Heat for Various Industrial Processes[36]

Aluminum production plants consume about 770 TBtu of energy per year. Production is divided between primary refining by Hall-Heroult cells and secondary production from recycled scrap. Due to operating furnace temperatures of about 1,290 °F, the primary cells have waste heat losses in the form of both off-gases and sidewall losses. Within secondary aluminum manufacturing, the furnaces can exhaust flue gases at temperatures between 2,000 and 2,200 °F.

Different from the various material production methods above, metal casting involves heating metal and pouring it into molds for goods like cars and pipes. Metal casting consumes about 257 TBtu per year and relies on furnaces with varying exhaust gas temperatures (most around 250-400 °F). Also different from typical manufacture processes are industrial boilers which consume about 6,500 TBtu of fuel annually. This industry relies on producing steam from boilers fueled by natural gas or byproduct fuels. The average exhaust temperatures are about 500 °F.

4.2.1.2 Steel Industry

While these industries account for a considerable amount of energy use and waste heat emission at a variety of temperatures and through a number of processes, we aim to focus on the iron and steel manufacturing industry due to its sizable energy use, about 1,900 TBtu per year, as well as

---

[36] Johnson, I.et al., 8.

its diversity of waste heat sources. Iron and steel manufacturing have five main stages: raw material processing, steel making and casting, hot rolling, cold rolling, and strip processing.[37]

Raw material processing involves preparing, measuring and analyzing the raw materials before combining them in a blast furnace. The raw materials include limestone, coal and iron. Limestone (CaCO3) is first converted to lime (CaO) via burning in a rotary lime kiln. Coal is converted to coke in a coke oven which heats the coal to 1,800 °F for up to 18 hours. [38] Next, the iron ore, coke and limestone are combined and charged into the top of a blast furnace. The blast furnace heats these ingredients by hot air at temperatures around 1,000-2,000 °F. This process creates pig iron, hot metal, and also offgas containing CO and CO2.[39] Once the hot metal is produced, it is incorporated in the next stage, the steel making process through either a Basic Oxygen Furnace (BOF) or Electric Arc Furnace (EAF).

Basic Oxygen Furnaces combine hot metal, steel scrap, and lime in a furnace to produce steel by oxidizing impurities in the raw materials. No external heat source is needed as the hot temperature required is produced by the exothermic reaction that occurs. This reaction also produces off-gases that are of high temperature but contain high levels of carbon monoxide (CO) and small concentrations of other contaminants. These gases are normally flared to the environment.[40]

Electric Arc Furnaces use electrical energy to heat recycled steel scrap and the other ingredients from the blast furnaces and create steel. The furnace is refractory lined and has a retractable roof that allows graphite electrodes to lower down and deliver electric arcs that generate heat and melt everything into liquid steel. The EAFs at Steel Dynamics, America's 4th largest steel company, process about 185 tons of scrap steel into 175 tons of liquid steel at 3,000 °F.[41] The difference in weight is due to the release of several gases and particulate emissions including CO, SO_x , NO_x, metal oxides, volatile organic compounds and pollutants. The temperatures of these emissions can range from 2,500-3,500 °F.[42] Throughout this process, cooling water is used to cool down the hot shell of the furnace and the off-gases as they travel from the EAF through ductwork to baghouses, which remove particulates from the gases and release the clean gas to the environment. By the time these emissions reach the baghouses, they are at about 250 °F.[43]

After the melted steel is made through BOF or EAF processes, it must be cast. Casting allows the liquid steel to cool into a solid rectangular slab. Although the slab is now solid, it can still be up to 1,750 °F and is about 75-155 feet long.[44]

The next stage of steel production is hot rolling. After the slab is made from the continuous rectangle produced in casting, it is reheated to about 2,000 °F. It is then squeezed between rollers

---

[37] Sinha-Spinks, T.

[38] "Interactive Steel Manufacturing Process."

[39] "Interactive Steel Manufacturing Process."

[40] Johnson, I.et al., 40

[41] Barry Schneider

[42] Johnson, I.et al., 41

[43] Barry Schneider

[44] Johnson, I.et al., 42

that make the steel thinner.[45] The steel is then rolled again during the cold rolling process in order to create precise shapes and increase the strength of the steel through strain hardening. This process is done at room temperature. Finally, the steel is processed, which can include pickling, galvanizing, and painting. Most of these processes require the steel to be reheated as well.

Thus, there are many different stages throughout steel production requiring high temperatures, there are many opportunities to harvest heat from the steel itself, equipment, or off-gases from furnaces. This makes it a strong option for applying our Stirling engine technology.

4.2.1.3 Implementation Within the Steel Industry

Due to the high waste heat temperature and feasibility of accessing the heated exhaust, electric arc furnaces (EAF) are a highly potential stage in which to implement the Stirling engine design (Figure 10). As mentioned above, the EAF heats steel to about 3000 °F in order to melt it, causing the molten steel released, the shell, the roof, and the exhaust gases to be very high temperature. The high temperature is dangerous to the furnace itself, so many factories use cooling water systems to cool the shell and roof of the furnace. While there are different types of cooling systems implemented, one involves panels of tubes that contain running water. In the Steel Dynamics plant, each EAF roof is cooled by water running across at about 2,500 gallons per minute. A large volume of water is used to cool the machinery and the water picks up about 10-15 °F from the hot roof.[46] This cooling water could potentially be a location for the hot side of the engine. The engine could be attached to the cooling panels, or the hot side could be inserted, using an airtight seal, into the pipes to have the hot water running over it. Since the cooling water temperature is not that high itself, the engine would need to run off a very low temperature differential.

A potentially more effective implementation scheme could be to use the exhaust gases as the hot side of the engine harnesses the heat from the exhaust stream leaving the EAF. While the gasses are also cooled by water within ductwork, they are still 250 °F by the time they reach the baghouses which expel them to the atmosphere.[47] The hot side of the engine could be placed within the ductwork carrying the gases, or a heat exchanger could be used to transfer the heat from the gases to the engine. The main concern with this approach is the abrasiveness of the exhaust, which contains CO, SO_x ,NO_x, metal oxides, volatile organic compounds and other pollutants.[48] Repeated exposure to this can harm equipment, increasing maintenance and repair costs. However, certain materials could be used to avoid and lessen damage.

---

[45] Johnson, I.et al., 45

[46] Barry Schneider.

[47] Barry Schneider.

[48] Johnson, I.et al., 41

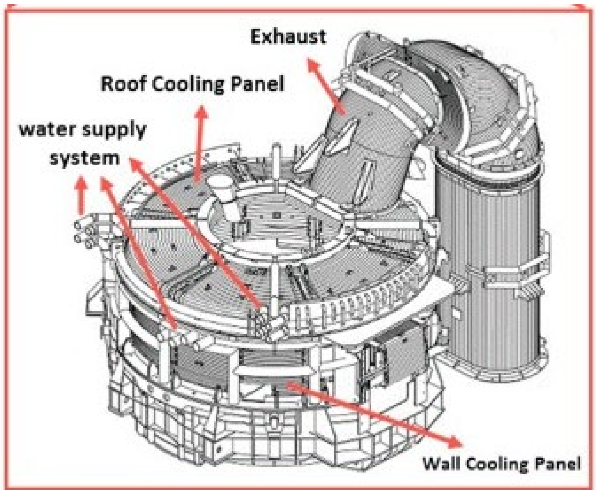

Figure 10: diagram of an Electric Arc Furnace.[49]

The next step in the implementation plan is to consider the cost of implementation, and maintenance in order to compare it to the energy savings and revenue benefits from the electricity production from the engine. Considering the case of the Steel Dynamics manufacturing plant, the following financial estimates are made. The plant has 4 EAF that each can melt a batch of about 185 tons of steel in 40 minutes.[50] In order to make comparisons between industries and based on our prototype, we assume that the Stirling engine is a 1 kW engine. Thus, if each EAF has a Stirling engine implemented and the plant runs about 10 batches per day, the engines would be able to produce about 26.67 kWh per day. Over a year, this would amount to about 9733 kWh. The electricity needed for each batch is about 400 kWh per ton, amounting to 74000 kWh per batch and 1080400 MWh per year.[51] Powering the EAFs alone would cost about $ 75 million per year with the cost of electricity for industries being about $0.07 per kWh.[52] The energy required even just to power the EAF is so great, that a 1 kW Stirling engine would not create any significant energy savings. Additionally, due to the energy intensive nature of the steel manufacturing processes, the electric grid for the plant is separate from the normal electric grid and is very complicated. Trying to get the power generated by the engine directly to the plant's grid would be costly and challenging. However, the energy generated by the engine could be sold back to the utility company or as a Renewable Energy Credit (REC). RECs allow households and companies that produce their own renewable energy, mainly solar, to sell it back to the electric grid if it is not used for their own needs. An approximate price for a REC is about $0.70. Each REC represents 1000 kWh of energy, thus with the annual energy production from the 1 kW Stirling engine set-up, the plant could earn about $6.81 per year.[53] In comparison to the large electricity costs of the plant, this is nothing, but with engines of a larger power output, the revenue could be more

---

[49] Khodabandeh et. al
[50] Barry Schneider.
[51] Martelaro, Nikolas
[52] "U.S. Energy Information"
[53] "U.S. Renewable Electricity Market."

impactful. These estimations also do not take into account other potential savings from government measures like tax incentives.

To improve the cost effectiveness of the Stirling engine in the steel industry application, we would need to scale up the energy production rate, which would increase both the revenue from REC and the energy savings from the plants own electricity consumption. This entails understanding the scaled-up production costs, with plans to mass produce the larger engines. Additionally, we would partner with political organizations in order to lobby for additional legislation involving tax credits and RECs to be increased. Finally, we would work with utilities to understand the necessary regulations and contracts necessary in order to sell the energy back to the main grid or implement it within the steel plant grid.

Overall, while there are still challenges to overcome, implementing our Stirling engine device in the steel industry or other industrial manufacturing processes would be an effective way to reduce the amount of waste heat released into the environment. Less waste means greater efficiency for the businesses which is a goal our society is always striving towards. Since the waste heat is captured and used to produce emission free electricity, the engine is a very competitive solution as it provides many environmental benefits. Manufacturing processes are very energy intensive, so the electricity provided by the engine could replace a portion of the plant electricity uses, decreasing the overall environmental impact of the plant. Producing the electricity from the already existing manufacturing processes also reduces the industrial plant's energy bill, an added benefit. Additional benefits can come from government incentives to reduce CO2 emissions.

4.2.2 Laundromats

Laundromats offer a novel application with great potential for the Stirling engine. Large-scale laundromats run commercially sized washing and drying machines that often run for 12 or 24 hours consecutively. While both washing and drying are energy intensive processes, drying specifically produces a lot of waste heat. This is where we believe Stirling engines could be implemented to produce electricity and reduce the operational monetary and carbon costs associated with running a large laundromat.

Depending on the type, drying machines can exhaust heat at temperatures up to 200^{O}F, which is around 90^{O}C.[54] The high temperature of exhaust provides a useful temperature differential for the Stirling engine. This application of the engine would be powered by the temperature differential between the exhaust heat and the outdoors. Because the temperature of dryer exhaust and the temperature of the outdoors will vary, the amount of power produced by the engine will vary as well. A better, higher temperature differential would likely occur in colder weather. For example, in Durham, North Carolina, the temperature varies from 30^{O}F to 90^{O}F, based on the time of day and time of year. This is equal to a range of about 0^{O}C, in colder weather, to 30^{O}C, in warmer weather. Therefore, the temperature differential between the dryer exhaust and the outside temperature that could be used by the engine would vary between up to 60^{O}C and up to 90^{O}C,

---

[54] Adhikari, Prakash

depending on the temperature outside. This engine would be implemented by placing the "hot" side near, but not blocking, the dryer vent.

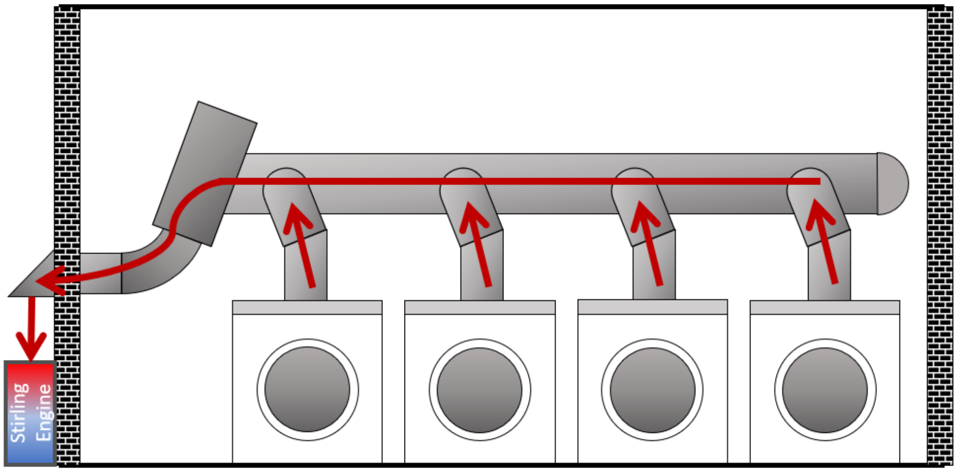

Figure 11: Diagram of a Stirling Engine Integrated with Laundromat Exhaust

Applying the Stirling engine to use waste heat generated by drying machines has benefits both to the environment and the customers who implement the engine in their business. The environment is benefited as the laundromat can use the clean energy that is produced by the engine instead of other, less clean sources of energy. In conjunction with the engine, a 5-kW commercial dryer would be able to recover 20% of its expended energy. Not only is this engine good for the environment, but it is good for the laundromat as well. Because they will save some energy by using the clean energy from the engine, they will in turn save money.

To determine if the amount of money that a laundromat would actually save per year, it was estimated that a drying machine in a laundromat runs for 13 hours a day, 6 days a week, and that energy costs 12¢ per kWh.[55, 56] Based on these assumptions, a 1-kW engine would save about $500 a year in energy savings.

Improving dryer efficiency is another way to save energy with regards to laundromats. However, the use of more efficient dryers do not mean that the Stirling engine would be rendered useless, because the efficiency of a dryer is not necessarily correlated with the temperature of the exhaust that it outputs.[57] Therefore, a Stirling engine will still be useful even as dryers improve in efficiency.

4.2.3 Applications Conclusion

Based on our initial findings, we believe that there are a number of potential applications for this type of Stirling engine. Certain application categories, such as industrial waste heat, provide the

---

[55] Adhikari, Prakash

[56] *Electric Choice*

[57] "Residential Clothes Dryers: A Closer Look at Energy Efficiency Test Procedures and Savings Opportunities"

benefit of large unused heat reservoirs. Others, such as laundromats and photovoltaics, also have sensible heat available.

However, these types of applications have temperature limits for efficient operation of their primary function. For example, laundry machines and solar panels become more energy intensive with increased temperatures. While the Stirling engine may benefit from this increase in temperature difference, it would be counterproductive to install a Stirling engine in this capacity, as the primary use of these sites becomes inefficient, cancelling out any benefit derived from a Stirling system installation.

Obviously, there are so many other applications that we were unable to consider in full. In addition to entirely novel uses, a major step forward for the application of Stirling engines will come when better means of transferring and storing unused heat become available. Technology, such as water cooling systems, that are able to quickly extract heat from the source (benefitting the source's operation efficiency), and facilitate the delivery of this heat to a Stirling engine will benefit the applicability of the engine type to an assortment of use cases.

4.2.4 Life Cycle Analysis of similar 1-kW Stirling engine

In order to quantify the net environmental and social impacts from the manufacture and operation of the engine, a cradle-to-gate life-cycle analysis was conducted. The analysis was based on an assumed 1-kW functional Stirling Engine unit and therefore components of the test setup were not included as part of the analysis. For process inputs this analysis looked at energy required for the transportation and manufacture of parts as well as the different materials used in construction. As an emissions-free form of electricity generation, CO2 equivalent emissions was selected as a key evaluation metric. Additionally, a weighted social impact metric, mPT, was examined in an attempt to gauge social benefits and costs. These two primary output metrics were estimated using the Sustainable Minds life cycle platform and database. The results from manufacturing were subsequently compared against the implied emissions avoided through alternative energy generation as well as the social impact estimates associated with operation. Additionally, ten different environmental impact categories were examined under the same platform in order to determine which potential ramifications from engine manufacture were the most significant (See Appendix J).

As the most viable business application under consideration, the laundromat dryer application mentioned in the section above was assumed for avoided emissions calculations. An expected ten-year lifespan for the engine was also assumed[58]. Because the applications were evaluated assuming a scaled 1 kW capacity, an existing life cycle analysis paper on a 1 kW Stirling Engine was selected as a case study for the analysis[59]. Additionally, approximations for part materials were made where necessary due to inventory limitations in the Sustainable Minds materials database.

---

[58] Stamford, L et.al p. 1124

[59] Stamford, L et. al

4.2.4.1 Life Cycle Results

The results of the life-cycle analysis indicated that the manufacture and transportation of parts for the engine resulted in an estimated 760kg CO2 equivalent emissions per completed engine. Roughly 75% of the emissions from manufacture derived from the production of the engine materials and 25% from energy used in the lifetime transportation of the materials. The avoided emissions from operation were estimated at 3,200 kg CO2 equivalent emissions per year, representing a net payback period of approximately 87 days, or less than three months. Additionally, over an expected ten-year operational lifetime, the overall emissions avoided translates to an estimated net reduction of 31,240 kg CO2 equivalent emissions.For the weighted social cost metric, the payback period from operation was determined to be longer, at approximately 4.7 years of operation in order to offset social costs from manufacture, but still a net social benefit over the ten-year operational lifetime.The most significant impact categories from engine manufacture were not emissions related but from potential carcinogenic byproducts from upstream manufacture of parts and as well as ecotoxicity from byproducts. This was later determined to be shared for many common manufacturing processes and not significant enough in magnitude to warrant concern.

4.3 Conclusions

The capture of waste heat in the built environment represents one viable approach in the context of a larger, multifaceted effort toward solving global energy and decarbonization problems. The conceptual free piston Stirling engine design is intended to demonstrate a feasible tool with the potential to utilize otherwise neglected waste heat as emission-free generation.

Seven main application categories for a 1 kW scaled Stirling engine were considered in this study. Of these applications under consideration, two candidate applications were eventually selected based on suitability for real world implementation. Preliminary analysis suggests that waste heat recovery from electric arc furnaces as well as laundromat dryers has the potential to generate electricity and reduce emissions with business models that are economical.

Success of the design is ultimately predicated on the construction and testing of a physical prototype. While we have taken initial steps towards this end, due to the COVID-19 crisis, physical assembly was not permitted within the time scale of this project. Testing of a manufactured prototype will allow the investigating team to confirm engine functionality, optimize engine performance, and extrapolate scaled power output and cycle efficiency. Until these data can be collected, assumptions made about engine scaling and power output are wholly speculative. Thus it is essential that a future team attempt to continue the manufacturing of the beta configuration free piston Stirling engine linear generator prototype to evaluate its feasibility as a solution to the problem of reclaiming low grade waste heat.

5 Appendix

5.1 Appendix A: Matlab Scripts

5.1.1 Engine Dynamics, Thermodynamics

```
clear;
format
close all
% Dynamics based on Equation of Motions based on Dr. Knight's book.
% Thermodynamics based on "Frequency-based design of a FPSE using genetic
% algorithm" by Sh. Zare; A.R Tavakolpour-Saleh. Referred to as "GA paper"

% 1-displacer
% 2-piston

%% Masses
m1=.18; % Displacer
m2=2.196; % Piston
%% Springs
k1=278; % Displacer  (1.59 lbs/in)
k2=487; % Piston-Displacer (2.78lbs/in) 487
k3=1399; % Piston (7.99 lbs/in)
%% Dampers
c1=10; % displacer
%c2=0.1;  %  displacer-piston,  assume  mostly  negligible  since  no  paper  found  ever  talks  about
estimating
c2=10; % piston

%% Geometry
d=8.89/100; % main diameter of piston in m (3.5in)
A_main=d^2*pi/4; %

dp=7.62/100; % diameter of piston in m ((3in))
Ap=dp^2*pi/4;


ddisp=7.62/100; % diameter of displacer in m (3 in)
ldisp=10.16/100; % length of displacer in m
Adisp=ddisp.^2*pi/4; % area of displacer in m

clearance_air=.5/1000;
A_air=(ddisp+2*clearance_air).^2*pi/4-Adisp;
Vr=(A_air)*ldisp; % volume between wall and regenerator/displacer

% dr=2.54/100; % diameterof rod in m
% Ar=dr^2*pi/4; % area of displacer rod


lho=3/100; % above displacer
Vho=(Adisp)*lho; % Equil Vol

lco=4/100; % below displacer
Vco=(Ap)*lco; % Equil Vol
%% Forcing
f=linspace(0,60,1e3);
Fo2=1; % seed value in N on piston
Fo1=0; % per paper, force acts on both. Same pressure acting on smaller area. In our configuration
this is set to zero
for i=1:length(f)
    omega(i)=2*pi*f(i);
    a11=-m1*(omega(i).^2)+(k1+k2)+j*(c1).*omega(i);
    a12=-k2;
    a21=-k2;
    a22=-m2*(omega(i).^2)+(k2+k3)+j*(c2)*omega(i);
```

```
    A_matrix=[a11 a12;
       a21 a22];
    b=[Fo1;
       Fo2];
    x(:,i)=A_matrix\b; % complex
    phase_piston_freq(i)=180/pi*angle(x(1,i)); % in deg
    phase_displacer_freq(i)=180/pi*angle(x(2,i)); % in deg
    phase_shift_freq(i)=abs(phase_displacer_freq(i)+phase_piston_freq(i)); % in deg
    if phase_shift_freq(i)>180
        phase_shift_freq(i)=360-phase_shift_freq(i);
    end
end

%% Frequency Study

figure (1)
clf
yyaxis left
plot(f,abs(x(1,:)))
title('Magnitude vs Forced Frequency')
hold on
plot(f,abs(x(2,:)))
xlabel('Frequency (Hz)')
yyaxis right
plot(f,phase_shift_freq)
legend('Displacer','Piston','Phase Shift')

%% Position over time
f=10; % in Hz
for p=1:15 % Number of iterations to tune Thermodynamic Force w/ Forcing amplitude
omega=[];
x=[];

       omega=2*pi*f;
    a11=-m1*(omega.^2)+(k1+k2)+j*(c1)*omega;
       a12=-k2;
       a21=-k2;
    a22=-m2*(omega.^2)+(k2+k3)+j*(c2)*omega;
       A_matrix=[a11 a12;
       a21 a22];
    b=[Fo1;
       Fo2];
    x=A_matrix\b; % complex
phase_piston=180/pi*angle(x(1,:)); % in deg
phase_displacer=180/pi*angle(x(2,:)); % in deg
phase_shift=abs(phase_displacer-phase_piston); % in deg
if phase_shift>180
    phase_shift=360-phase_shift;
end
% plot motion
figure(2)
clf
t=linspace(0,1,1e3);
hold on
piston_motion=abs(x(2))*sin(2*pi*f*(t));
disp_motion=abs(x(1))*sin(2*pi*f*(t)-(phase_shift)*pi/180);

plot(t,piston_motion)
plot(t,disp_motion)
legend('Piston','Displacer')

amplitude_ratio=abs((x(1)/x(2)))
axis([0 1 -1.15*max([ abs(x(2)) abs(x(1))]) 1.15*max([abs(x(2)) abs(x(1))])])
title('Piston & Displacer dynamics')
xlabel('time (s)')
ylabel('Displacement (m)')

% just for reporting
dim = [.2 .63 .2 .3];
str = ['Piston Forcing Amplitude=',num2str(abs(round(Fo2))),'N','       ',...
```

```
    'Phase Shift=',num2str(round(phase_shift)),'deg','    ',...
    'Frequency=',num2str(round(f)),'Hz'];
annotation('textbox',dim,'String',str,'FitBoxToText','off','LineStyle','none');

%% Thermodynamics
% Temperature & Equil Vols
Th=500; % in hot space
Tc=300; % in cold space
Tr=(Th-Tc)/log(Th/Tc); % in regenerator

Po=1*1e5; % 1 bar
MW=4/1000;  % in kg/mol, He
Troom=300; % room temp loading
M=(Vho+Vco+Vr)*Po*(MW)/(8.314*Troom); % for ideal gas (i.e not air) ; mass in kg, paper neglected
Vr I
%think
%M=(Vho+Vco)*1.224; % for air, room temp density=1.224; % mass in kg, paper neglected Vr I think
just by looking at their number
%R=MW/8.314;

% Find Amplitude of Pressure
Vhx=Vho-(Adisp)*disp_motion; % expression from paper
Vcx=Vco+(Adisp)*(disp_motion)-(Ap)*(piston_motion); % expressions from paper

P_inst=M*(8.314/MW)./((Vhx/Th)+(Vcx/Tc)+(Vr/Tr));

Force=(P_inst-Po)*(Ap);

Mean_F=abs(mean(Force))


Fo2=Mean_F; % on piston
Fo1=0; %(same pressure acting on smaller area)


p=p+1;
end

figure(3)
clf
yyaxis left
plot(t,Po*ones(1,length(t)))
hold on
plot(t,P_inst)
axis([0 1 .8*Po 1.1*max(P_inst)])
xlabel('time(s)')
ylabel('Pressure (Pa)')

yyaxis right
plot(t,Vhx,t,Vcx)
legend('Charge Pressure','Working Pressure','Hot Volume','Cold Volume')
ylabel('Volume (m3)')
title('Thermodynamics')

figure(4)
%clf
Vol=Vcx+Vhx;
P=P_inst-Po;
plot(Vol,P_inst)
ylabel('Pressure (Pa)')
xlabel('Volume (m3)')
title('P-V')

Power=round(abs(trapz(Vol(1:101),P(1:101)))*f,0) % in W (range is for one period 0-->0.1s)
% Volumemin=Vr+min(Vcx)+min(Vhx)
% Volumemax=Vr+max(Vcx)+max(Vhx)

%% Results from SW
T=readtable('Moredots_FPSE.xlsx','Sheet',1,'Range','A4:D605');
range=300:331; % 98:1:109; 40:1:51
```

```
disp_SW=T.Ref_CoordinateSystem__1(range)/1000;
piston_SW=T.Ref_CoordinateSystem_(range)/1000;

Vhx_SW=Vho-(Adisp)*(disp_SW-mean(disp_SW)); % expression from paper
Vcx_SW=Vco+(Adisp)*(disp_SW-mean(disp_SW))-(Ap)*(piston_SW-mean(piston_SW)); % expressions from
paper

P_inst_SW=M*(8.314/MW)./((Vhx_SW/Th)+(Vcx_SW/Tc)+(Vr/Tr));
figure(4)
hold on
plot(Vhx_SW+Vcx_SW,P_inst_SW,'r*-')
legend('Matlab Simulation','SolidWorks Simulation','EdgeColor','None')
Power_SW=round(trapz(Vhx_SW+Vcx_SW,P_inst_SW)*f,0)

figure(2)
plot(T.Time,(T.Ref_CoordinateSystem_-mean(T.Ref_CoordinateSystem_))/1000,'b*-')
hold on
plot(T.Time,(T.Ref_CoordinateSystem__1-mean(T.Ref_CoordinateSystem__1))/1000,'r*-')
axis([0 2 -1.15*max([ abs(x(2)) abs(x(1))]) 1.15*max([abs(x(2)) abs(x(1))])])

figure(6)
Vol=Vcx+Vhx;
P=P_inst-Po;
plot(Vcx,P_inst,'b-')
hold on
plot(Vcx_SW,P_inst_SW,'b*-')
plot(Vhx,P_inst,'r-')
plot(Vhx_SW,P_inst_SW,'r*-')
legend('Matlab Cold Volume','SW Cold Volume','Matlab Hot Volume','SW Hot Volume')
ylabel('Pressure (Pa)')
xlabel('Volume (m3)')
```

5.1.2 Coil generator calculations

```
clear;
amp=13.8; % piston amplitude in mm
w=28.75/1000; % width of slot (3.5''(outer diameter)-1''(inner diameter))/2-3mm (inner wall
thickness)-
h=(6.35+2*amp)/1000; % height of slot (for calculation (amp x2+height of magnet), but make 5 cm
for construction, alignment purposes and allows extra turns)
g=0.66802/1000; % AWG 22 enameled (per Amazon)
k=0.6; % filling factor (wire guide says 0.9, constructed one in literature gave 0.8); essentially
an indication of how good we are at winding coil
Nmax=floor(w*h*k/(g^2)) % max number of windings in designed slot

layer_height=floor(h/g);
layer_width=floor(Nmax/layer_height);

diameter_first=2.54/100+2*3/1000; %inner diameter+2xwall thickness
diameter_last=2.54/100*3.5; % outer diameter
x_dia=linspace(diameter_first,diameter_last,layer_width);
n=0;
for i=1:layer_width
    A(i)=pi/4*(x_dia(i))^2;
    n=n+1;
end
total_length=ceil(Nmax/layer_width*pi*mean([diameter_first diameter_last])) % in m
% Magnet
Br=1.375; % in T
inner_diameter=1/4*2.54/100; % inner diameter
outer_diameter=1*2.54/100; % outer diameter
Am=pi/4*(outer_diameter^2-inner_diameter^2); % magnet area
%% Coil
Resistance=52.9392/1000*total_length; % AWG 22 resistance per 1000 m
skin_depth=10/1000; % copper at 10 Hz, obtained online, a measurement of how much can a magnetic
field penetrate into a conductor (coil in this case)
f=10; % Hz

% Method 1 (Using Changing area & magnetic flux, carrying out integration).
```

```
% developed using emf=N*dB*f where N is number of coils and dB is integrated
% flux across each concentric area around the magnet, with understanding
% magnetic field B decreases exponentially radially as it penetrates into
% coil ("skin effect"). Can cite physics 2 book
x_rad=x_dia/2; % radii
B_1=Br.*exp(-x_rad/skin_depth); % adjusted for B=Br at magnet's inner edge (6.35mm)
figure(1)
clf
plot(x_rad*100/2.54,B_1)
xlabel('Radial Distance from Magnet(in)')
ylabel('Magnetic Field Strength (T)')
flux_change=trapz(A,B_1);
emf_exp_method1=floor(Nmax*flux_change*f) % in V, no load emf

% Method 2 (from Romanian Paper, found in google drive)

B_2=Br;
emf_exp_method2=floor(Nmax*B_2*Am*f) % in V, no load emf this method was the one used by Romanian
paper (found in drive)

% Power Output for "5-9V" no load emf would be 1-3W (200-300mA); per online
% forum of a similar sized linear generator with that range of voltage and
%   "1-10Hz"   mentioned.   Not   a   citable   source   but   couldnt   find   much   else.
https://cr4.globalspec.com/thread/122436/DIY-Magnetic-Linear-Electricity-Generator

%% Power
% Use more conservative estimate
mu=4*pi*1e-7;
B_1_mean=min((B_1));
H_1=B_1_mean./mu;

lm=(2.54/100)/2*pi;
i_est1=H_1*lm/Nmax

P_out=emf_exp_method1*i_est1-i_est1^2*Resistance
```

5.2 Appendix B: Maple Code for Static Geometry Calculation

Chris Orrico
Stirling Engine Spring Calcs/Equilibrium Solutions - 2/4/2020
All Values in SI unless otherwise stated

Prepare Worksheet

```
> restart;
```

Solve for displacement given k's

```
> Vals := g = 9.8, mp = 2.2, md = 0.18, k1 = 1388, k2 = 485, k3 = 275.3, d1 = 0.0122, d2 = 0.035,
      d3 = 0.0617;
```

$$Vals := g = 9.8, mp = 2.2, md = 0.18, k1 = 1388, k2 = 485, k3 = 275.3, d1 = 0.0122, d2 = 0.035, d3 = 0.0617 \tag{1}$$

```
>
```

```
> pistonEq := k1·(x1 + d1) = mp·g + k2·(d2 + x2 − x1) ;
```

$$pistonEq := k1\ (x1 + d1) = mp\, g + k2\ (d2 + x2 - x1) \tag{2}$$

```
> displacerEq := k2·(d2 + x2 − x1) = md·g + k3·(d3 − x2);
```

$$displacerEq := k2\ (d2 + x2 - x1) = md\, g + k3\ (d3 - x2) \tag{3}$$

```
> xSoln := simplify(expand(solve( {pistonEq, displacerEq}, [x1, x2])))
```

$$xSoln := \left[\left[x1 = \frac{((d2 + d3)\ k3 - k1\ d1 + g\ (md + mp))\ k2 + k3\ (-k1\ d1 + mp\, g)}{(k1 + k3)\ k2 + k1\ k3}, x2 = \frac{((-d1 - d2)\ k1 + k3\ d3 + g\ (md + mp))\ k2 + k1\ (k3\ d3 + md\, g)}{(k1 + k3)\ k2 + k1\ k3}\right]\right] \tag{4}$$

```
> xVals := subs(Vals, xSoln)
```

$$xVals := [[x1 = 0.01453918115, x2 = 0.01160925012]] \tag{5}$$

5.3 Appendix C: Modelling

Table 7: Input parameters to MATLAB model

Parameter		**Value**
Dynamic		
	Frequency (*f*)	10 Hz
	Displacer Mass (m_1)	0.18 kg
	Piston Mass (m_2)	2.196 kg
	Displacer spring (k_1)	278 N/m
	Piston-Displacer spring (k_2)	487 N/m
	Piston spring (k_3)	1399 N/m
Geometric		
	Main diameter (d)	7.62 cm (3.5’’)
	Length of displacer/regenerator space (l_{disp})	10.16 cm (4’’)
	Equilibrium length of hot space (l_{ho})	3 cm
	Equilibrium length of cold space (l_{co})	4 cm
Thermodynamic		
	Hot temperature (T_h)	500K (227℃)
	Cold temperature (T_c)	300K (27℃)
	Gas & bounce pressure (P_b)	Helium (1 bar)

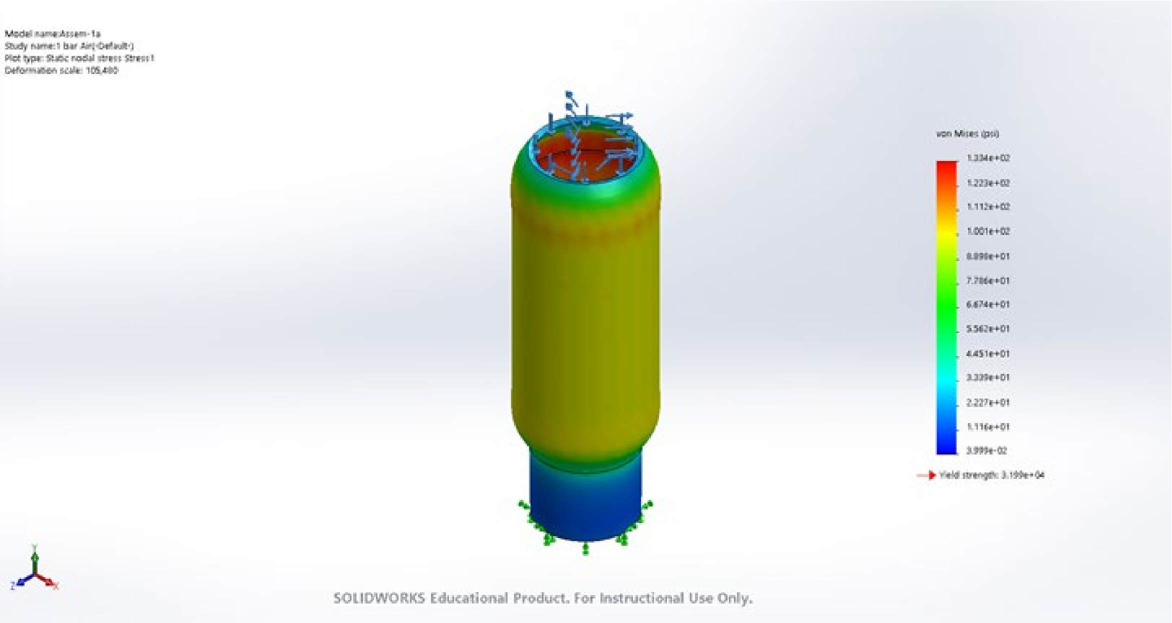

Figure 12: FEA study from internal pressure stresses

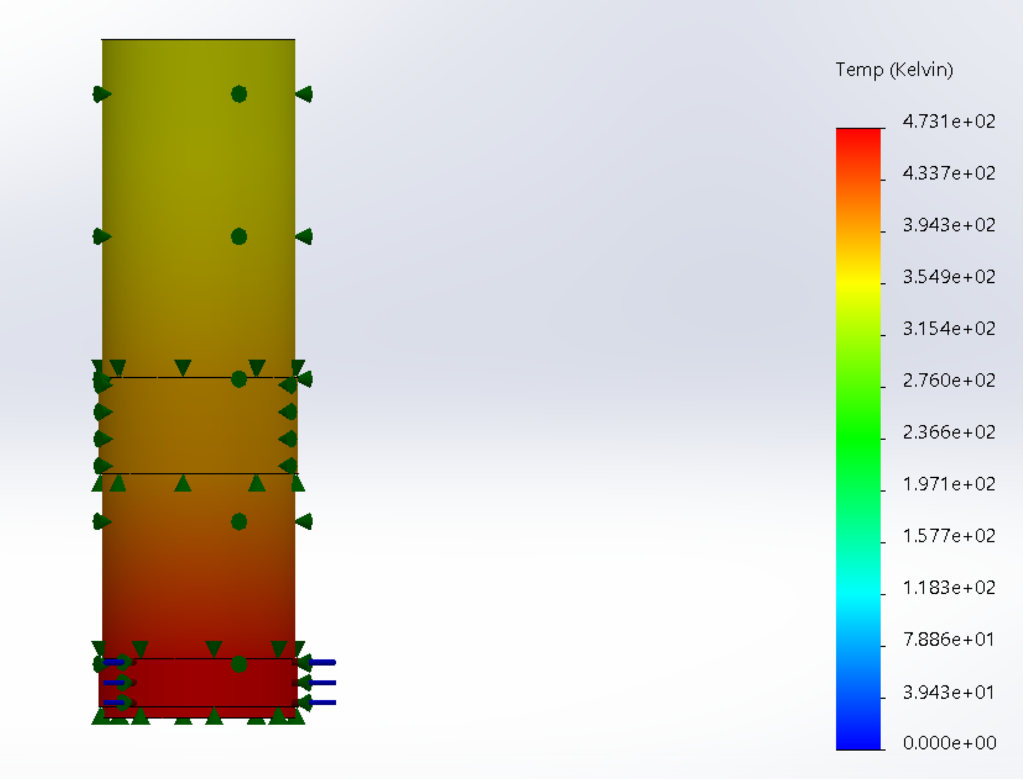

Figure 13: Thermal Study with no external cooling

5.4 Appendix D: CAD SolidWorks Model

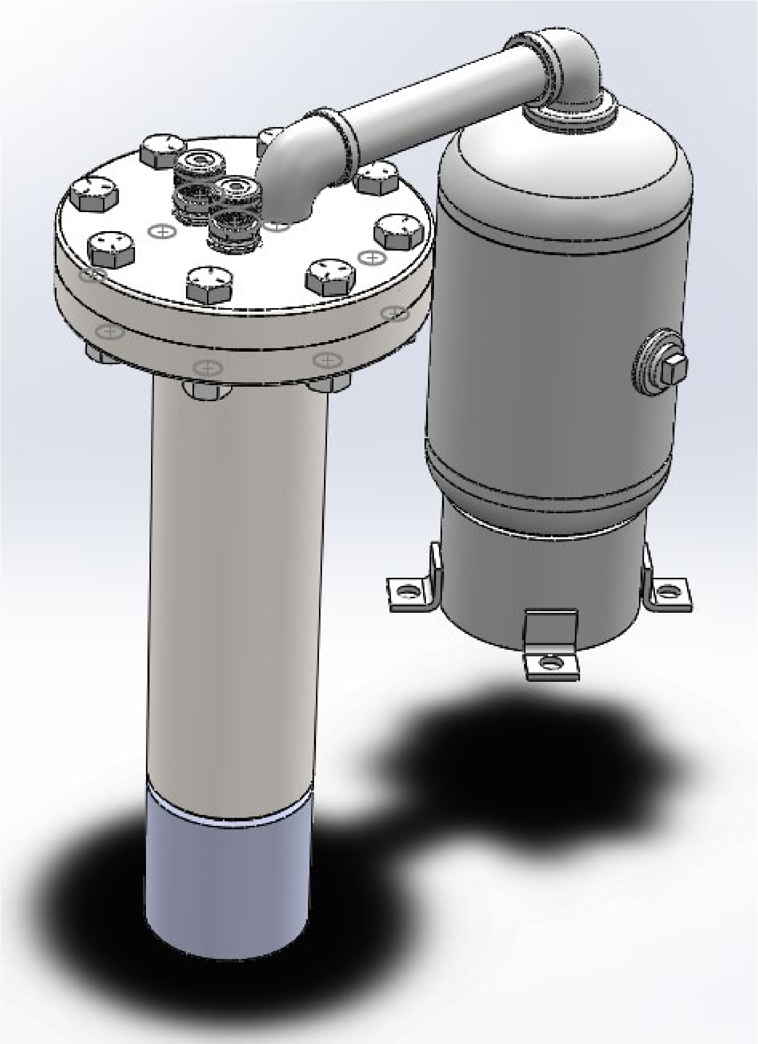

Figure 14: CAD Model, Solid

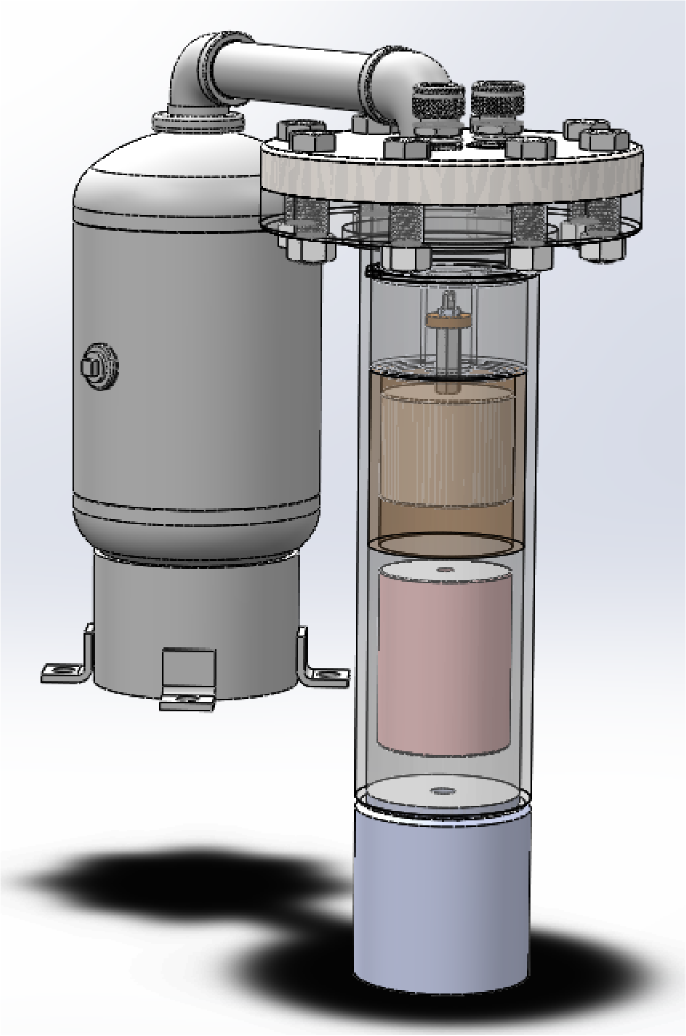

Figure 15: CAD Model, Transparent

5.5 Appendix E: Technical Drawings

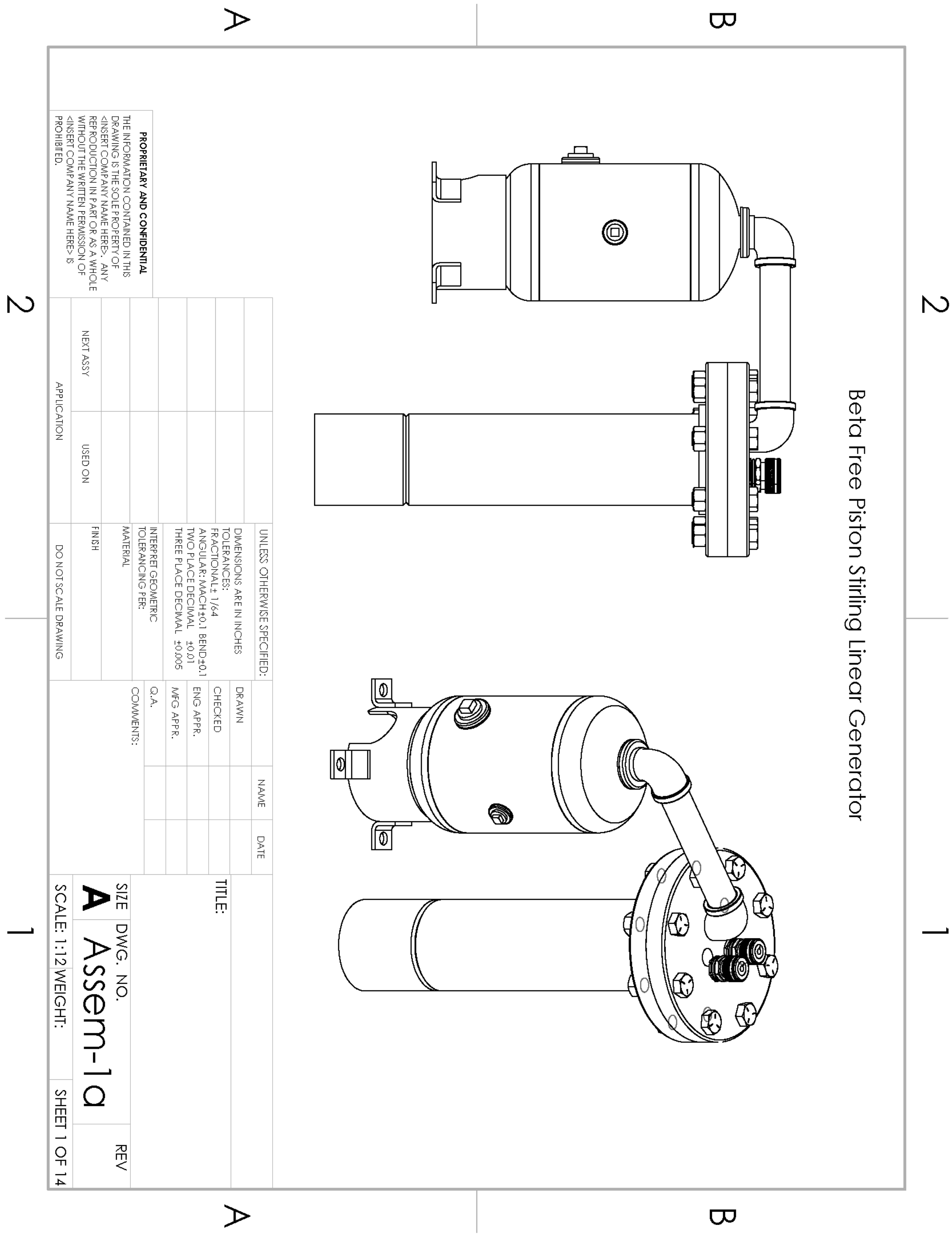

Beta Free Piston Stirling Linear Generator

ITEM NO.	PART NUMBER	QTY.
1	EndPlug-1a	1
2	RegeneratorStructure-1a	1
3	6391K471	1
4	DisplacerCylinder-1a	1
5	DisplacerStructureBot-1a	1
6	DisplacerStructureTop-1a	1
7	9634K31	4
8	Piston-1a	1
9	93505A199	1
10	3360K862	1
11	9634K23	2
12	91947A110	1
13	GeneratorHousing-1a	1
14	Cylinder-1a	1
15	pipefittingsdirect.com SKU: KFSO3.5	1
16	99142A670	1
17	CapFlange	1
18	44605K225	1
19	1584K1	1
20	44605K136	2
21	44615K526	1
22	Grainger 24C155	2
23	91247A438	8
25	95462A535	8
25	92147A035	8

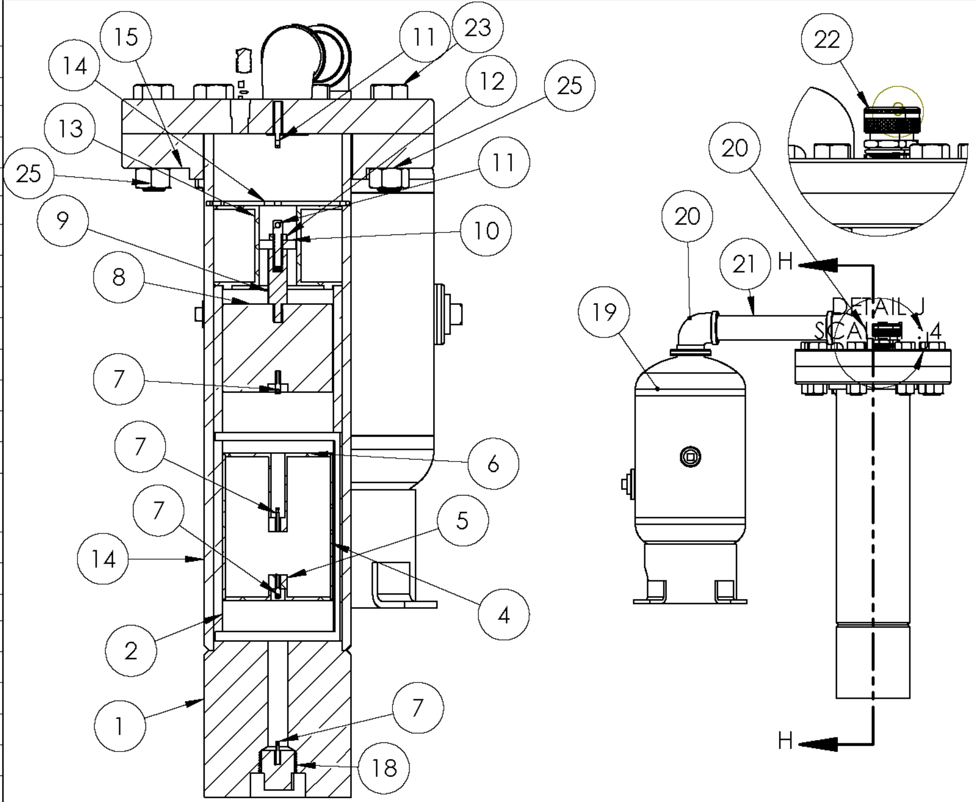

SECTION H-H
SCALE 1 : 4

2
1
B
A

UNLESS OTHERWISE SPECIFIED:
DIMENSIONS ARE IN INCHES
TOLERANCES:
FRACTIONAL±
ANGULAR: MACH± BEND ±
TWO PLACE DECIMAL ±
THREE PLACE DECIMAL ±

INTERPRET GEOMETRIC
TOLERANCING PER:
MATERIAL
FINISH

	NAME	DATE
DRAWN		
CHECKED		
ENG APPR.		
MFG APPR.		
Q.A.		

COMMENTS:
All item numbers from McMaster Carr unless otherwise stated

TITLE:
Assembly Part Reference

SIZE A
DWG. NO. Assem-1a
REV
SCALE: 1:12 WEIGHT: SHEET 2 OF 14

PROPRIETARY AND CONFIDENTIAL

THE INFORMATION CONTAINED IN THIS DRAWING IS THE SOLE PROPERTY OF <INSERT COMPANY NAME HERE>. ANY REPRODUCTION IN PART OR AS A WHOLE WITHOUT THE WRITTEN PERMISSION OF <INSERT COMPANY NAME HERE> IS PROHIBITED.

NEXT ASSY
USED ON
APPLICATION
DO NOT SCALE DRAWING

ITEM NO.	PART NUMBER	DESCRIPTION	QTY.
1	7767T77	Low-Carbon Steel Round Tube	1

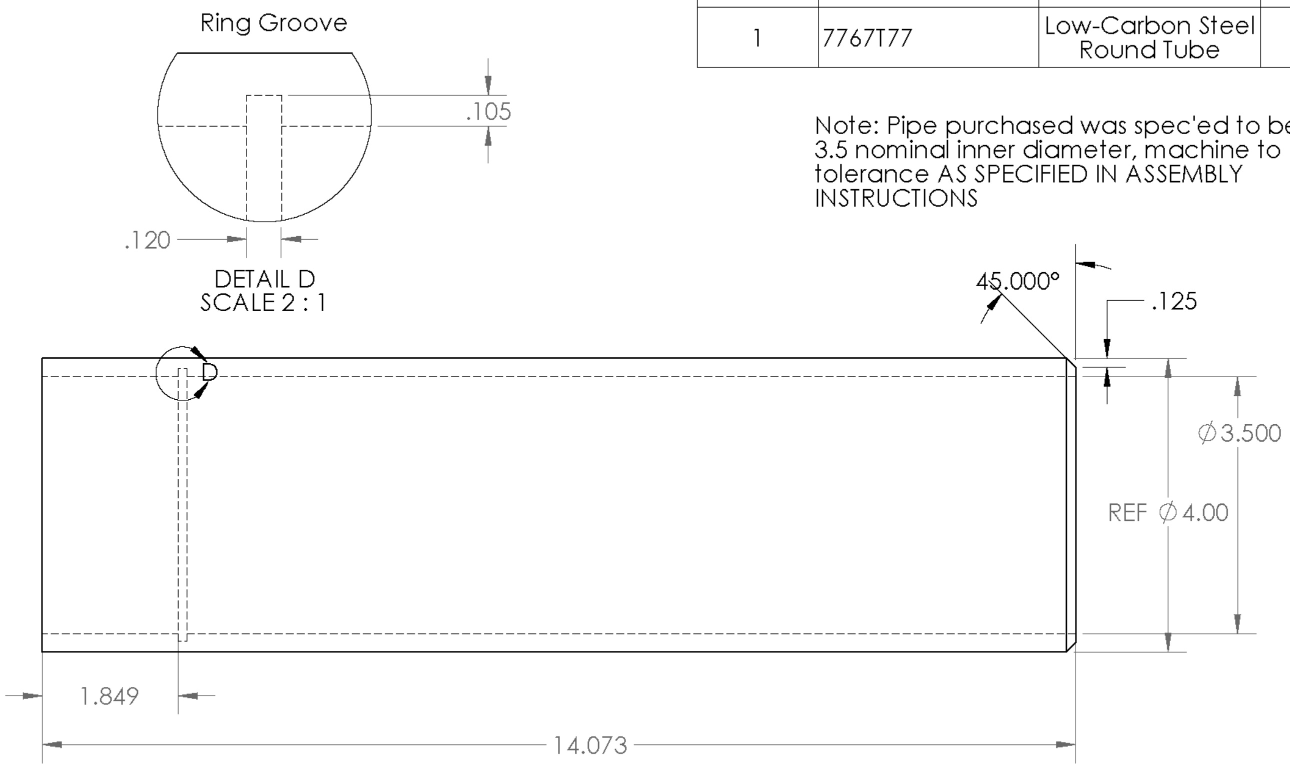

Note: Pipe purchased was spec'ed to be 3.5 nominal inner diameter, machine to tolerance AS SPECIFIED IN ASSEMBLY INSTRUCTIONS

UNLESS OTHERWISE SPECIFIED:
DIMENSIONS ARE IN INCHES
TOLERANCES:
FRACTIONAL±
ANGULAR: MACH± BEND ±
TWO PLACE DECIMAL ±0.01
THREE PLACE DECIMAL ±0.005
INTERPRET GEOMETRIC TOLERANCING PER:
MATERIAL
Low Carbon Steel
FINISH
DO NOT SCALE DRAWING

	NAME	DATE
DRAWN		
CHECKED		
ENG APPR.		
MFG APPR.		
Q.A.		

COMMENTS:

NEXT ASSY
USED ON
APPLICATION

TITLE:
Cylinder-1a

SIZE
A
DWG. NO.
Assem-1a
REV
SCALE: 1:4
WEIGHT:
SHEET 3 OF 14

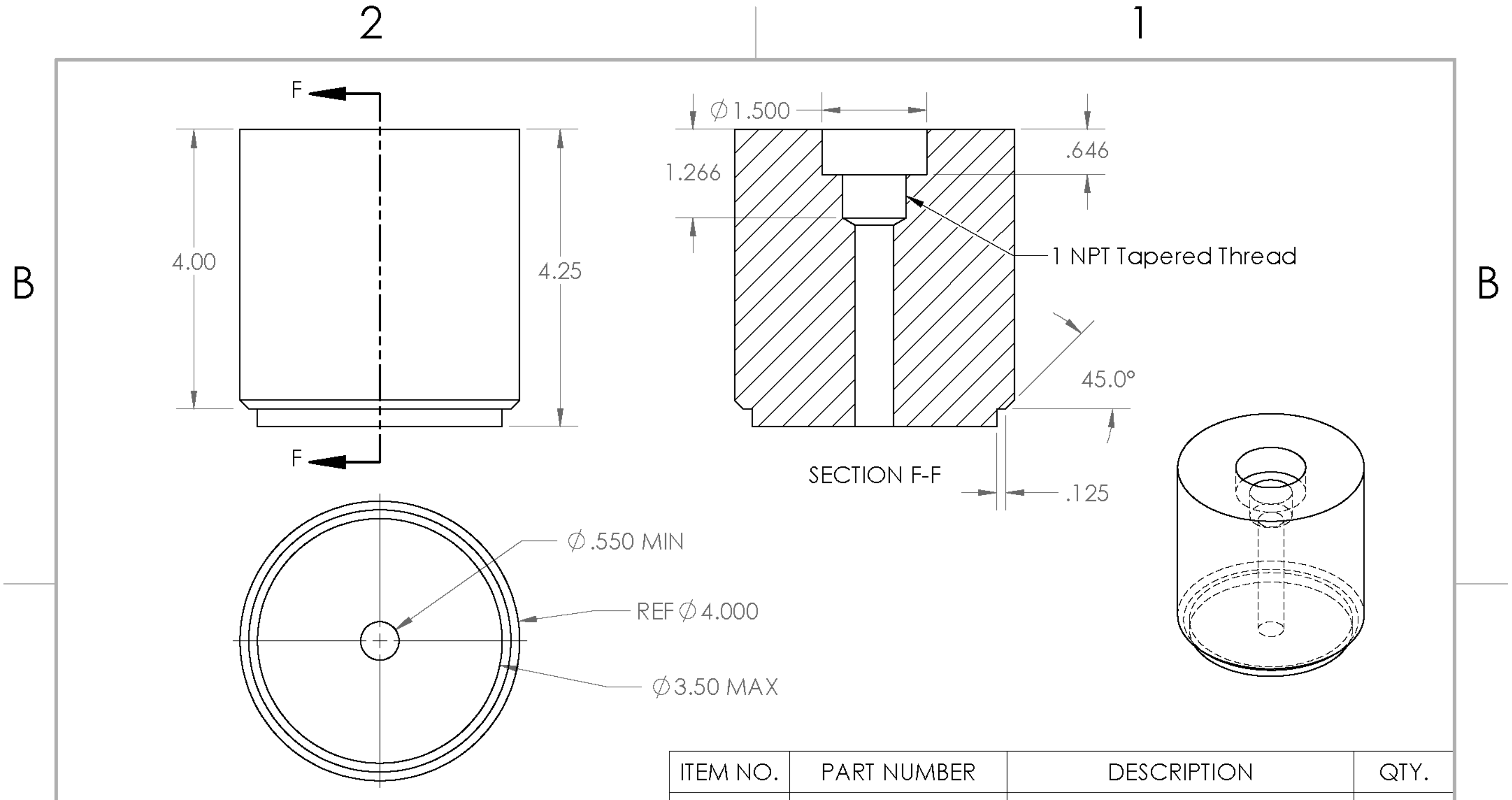

ITEM NO.	PART NUMBER	DESCRIPTION	QTY.
1	7786t58	Low-Carbon Steel Disc	1

PROPRIETARY AND CONFIDENTIAL

THE INFORMATION CONTAINED IN THIS DRAWING IS THE SOLE PROPERTY OF <INSERT COMPANY NAME HERE>. ANY REPRODUCTION IN PART OR AS A WHOLE WITHOUT THE WRITTEN PERMISSION OF <INSERT COMPANY NAME HERE> IS PROHIBITED.

NEXT ASSY	USED ON
APPLICATION	

UNLESS OTHERWISE SPECIFIED:
DIMENSIONS ARE IN INCHES
TOLERANCES:
FRACTIONAL±
ANGULAR: MACH± BEND ±
TWO PLACE DECIMAL ±0.01
THREE PLACE DECIMAL ±0.005
INTERPRET GEOMETRIC TOLERANCING PER:
MATERIAL
Low Carbon Steel
FINISH
DO NOT SCALE DRAWING

	NAME	DATE
DRAWN		
CHECKED		
ENG APPR.		
MFG APPR.		
Q.A.		

COMMENTS:

TITLE:
EndPlug-1a

SIZE
A
DWG. NO.
Assem-1a
REV

SCALE: 1:2
WEIGHT:
SHEET 4 OF 14

ITEM NO.	PART NUMBER	DESCRIPTION	QTY.
1	44605K225	Low-Pressure Pipe Fitting Steel, Solid Plug with External Square Drive, 3/4 NPT	1

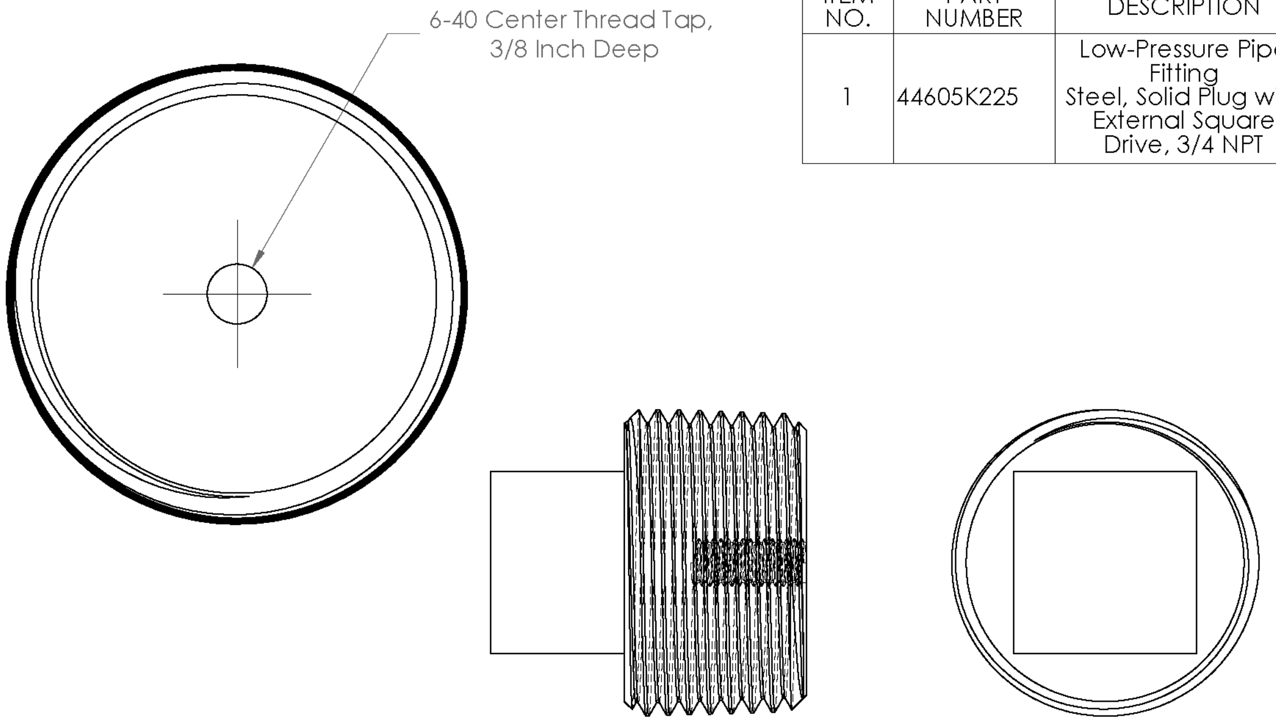

PROPRIETARY AND CONFIDENTIAL

THE INFORMATION CONTAINED IN THIS DRAWING IS THE SOLE PROPERTY OF <INSERT COMPANY NAME HERE>. ANY REPRODUCTION IN PART OR AS A WHOLE WITHOUT THE WRITTEN PERMISSION OF <INSERT COMPANY NAME HERE> IS PROHIBITED.

NEXT ASSY	USED ON
APPLICATION	

UNLESS OTHERWISE SPECIFIED:
DIMENSIONS ARE IN INCHES
TOLERANCES:
FRACTIONAL±
ANGULAR: MACH± BEND ±
TWO PLACE DECIMAL ±
THREE PLACE DECIMAL ±
INTERPRET GEOMETRIC TOLERANCING PER:
MATERIAL
FINISH
DO NOT SCALE DRAWING

	NAME	DATE
DRAWN		
CHECKED		
ENG APPR.		
MFG APPR.		
Q.A.		

COMMENTS:

TITLE:

End Plug Pipe Fitting

SIZE A
DWG. NO. Assem-1a
REV
SCALE: 2:1
WEIGHT:
SHEET 5 OF 14

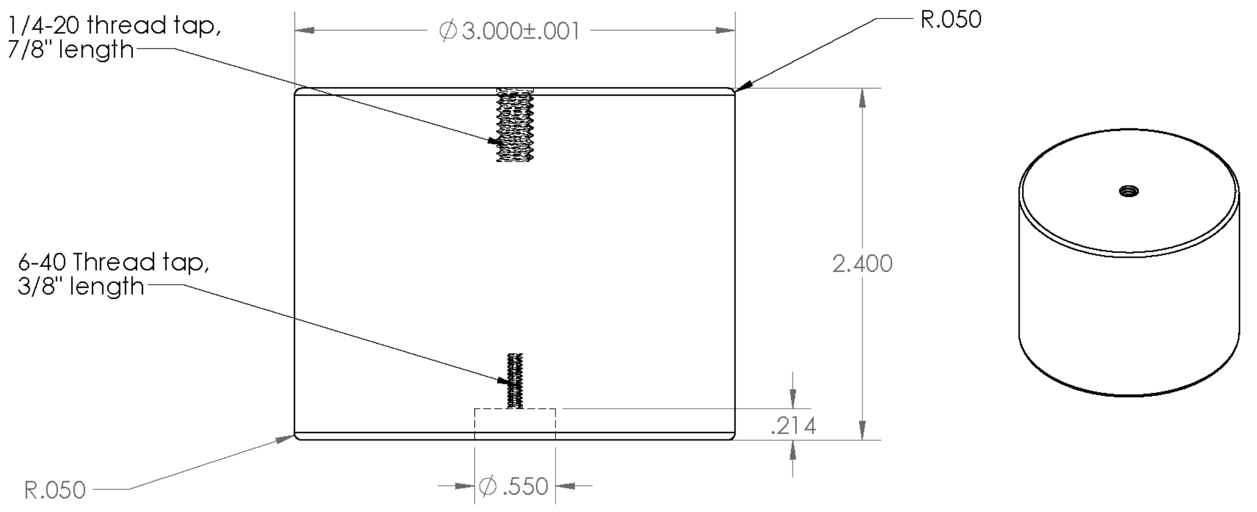

ITEM NO.	PART NUMBER	DESCRIPTION	QTY.
1	7786T36	Low-Carbon Steel Disc	1

PROPRIETARY AND CONFIDENTIAL

THE INFORMATION CONTAINED IN THIS DRAWING IS THE SOLE PROPERTY OF <INSERT COMPANY NAME HERE>. ANY REPRODUCTION IN PART OR AS A WHOLE WITHOUT THE WRITTEN PERMISSION OF <INSERT COMPANY NAME HERE> IS PROHIBITED.

NEXT ASSY
USED ON
APPLICATION

UNLESS OTHERWISE SPECIFIED:
DIMENSIONS ARE IN INCHES
TOLERANCES:
FRACTIONAL±
ANGULAR: MACH± BEND ±
TWO PLACE DECIMAL ±0.01
THREE PLACE DECIMAL ±0.005
INTERPRET GEOMETRIC TOLERANCING PER:
MATERIAL
FINISH
DO NOT SCALE DRAWING

	NAME	DATE
DRAWN		
CHECKED		
ENG APPR.		
MFG APPR.		
Q.A.		

COMMENTS:

TITLE:
Piston-1a

SIZE A
DWG. NO. Assem-1a
REV
SCALE: 1:2
WEIGHT:
SHEET 6 OF 14

NOTE: DIMENSIONS MARKED NOMINAL SHOULD
BE REDIMENSIONED UPON MEASUREMENT OF THE
REAL INNER DIAMETER OF REGENERATORSTRUCTURE-1A
FOR H8/f7 CLOSE RUNNING CLEARANCE FIT

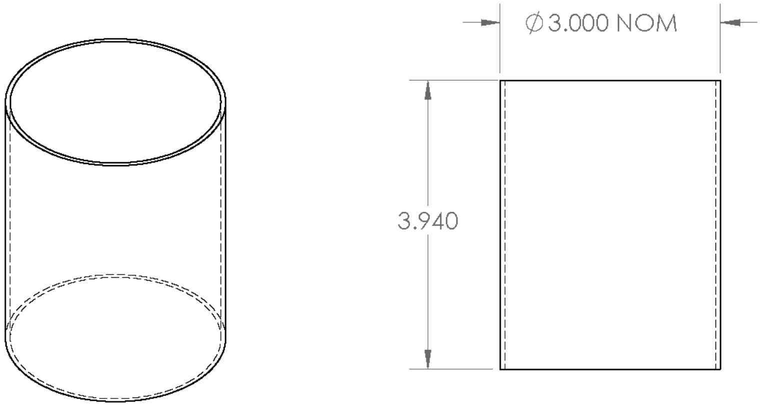

Note: Displacer Top and Bottom Cap will reference measured ID of purchased round tube

ITEM NO.	PART NUMBER	DESCRIPTION	QTY.
1	9056K85	Multipurpose 6061 Aluminum Round Tube 0.065" Wall Thickness, 3" OD	1

PROPRIETARY AND CONFIDENTIAL

NEXT ASSY
USED ON
APPLICATION

UNLESS OTHERWISE SPECIFIED:
DIMENSIONS ARE IN INCHES
TOLERANCES:
FRACTIONAL±
ANGULAR: MACH± BEND ±
TWO PLACE DECIMAL ±0.01
THREE PLACE DECIMAL ±0.005
INTERPRET GEOMETRIC TOLERANCING PER:
MATERIAL
6061 Aluminum
FINISH
DO NOT SCALE DRAWING

	NAME	DATE
DRAWN		
CHECKED		
ENG APPR.		
MFG APPR.		
Q.A.		

COMMENTS:

TITLE:
DisplacerCylinder-1a

SIZE A
DWG. NO. Assem-1a
REV
SCALE: 1:2
WEIGHT:
SHEET 7 OF 14

NOTE: DIMENSIONS MARKED NOMINAL SHOULD
BE REDIMENSIONED UPON MEASUREMENT OF THE
REAL INNER DIAMETER OF REGENERATORSTRUCTURE-1A
(FOR THE 2.992 NOM DIAMETER) AND THE REAL
INNER DIAMETER OF DISPLACERCYLINDER-1A (2.870 NOM).
THESE SHOULD BE A H8/f7 CLOSE RUNNING FIT AND A
H7/h6 LOCATIONAL CLEARANCE FIT, RESPECTIVELY

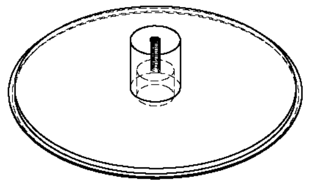

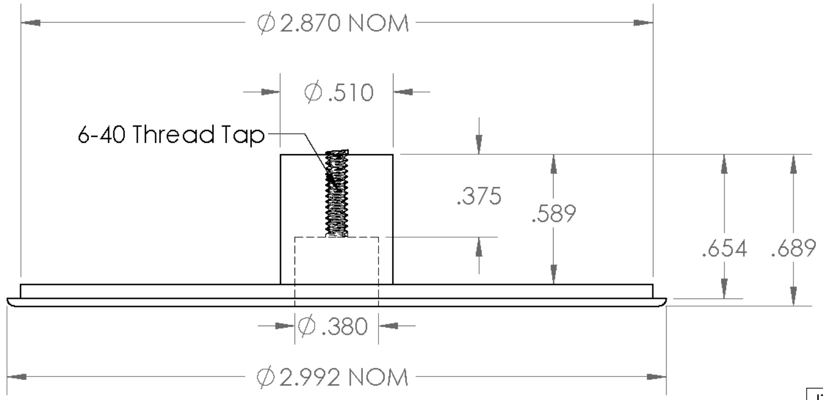

ITEM NO.	PART NUMBER	DESCRIPTION	QTY.
1	1610T19	Multipurpose 6061 Aluminum 3" Diameter, 1" Length	1

PROPRIETARY AND CONFIDENTIAL

THE INFORMATION CONTAINED IN THIS DRAWING IS THE SOLE PROPERTY OF <INSERT COMPANY NAME HERE>. ANY REPRODUCTION IN PART OR AS A WHOLE WITHOUT THE WRITTEN PERMISSION OF <INSERT COMPANY NAME HERE> IS PROHIBITED.

NEXT ASSY	USED ON
APPLICATION	

UNLESS OTHERWISE SPECIFIED:

DIMENSIONS ARE IN INCHES
TOLERANCES:
FRACTIONAL±
ANGULAR: MACH± BEND ±
TWO PLACE DECIMAL ±.01
THREE PLACE DECIMAL ±.005

INTERPRET GEOMETRIC TOLERANCING PER:

MATERIAL
6061 Aluminum

FINISH

DO NOT SCALE DRAWING

	NAME	DATE
DRAWN		
CHECKED		
ENG APPR.		
MFG APPR.		
Q.A.		

COMMENTS:

TITLE:

DisplacerStructureBot-1a

SIZE	DWG. NO.	REV
A	Assem-1a	

SCALE: 1:1 WEIGHT: SHEET 8 OF 14

ITEM NO.	PART NUMBER	DESCRIPTION	QTY.
1	1610T19	Multipurpose 6061 Aluminum, 3" Diameter Round, 3" Length	1

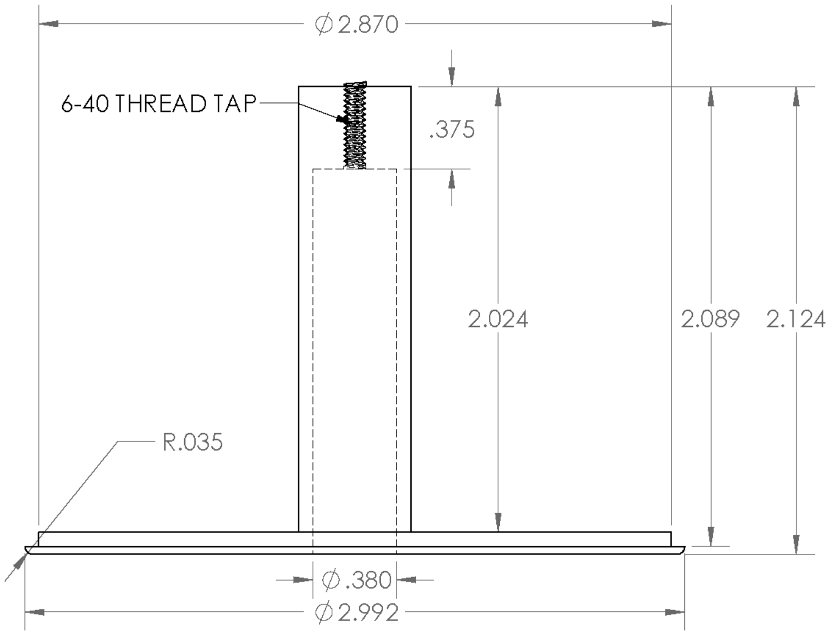

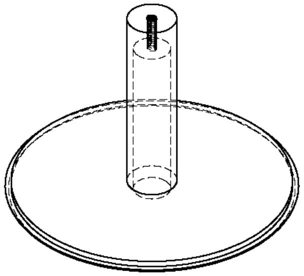

NOTE: DIMENSIONS MARKED NOMINAL SHOULD BE REDIMENSIONED UPON MEASUREMENT OF THE REAL INNER DIAMETER OF REGENERATORSTRUCTURE-1A (FOR THE 2.992 NOM DIAMETER) AND THE REAL INNER DIAMETER OF DISPLACERCYLINDER-1A (2.870 NOM). THESE SHOULD BE A H8/f7 CLOSE RUNNING FIT AND A H7/h6 LOCATIONAL CLEARANCE FIT, RESPECTIVELY

UNLESS OTHERWISE SPECIFIED:

DIMENSIONS ARE IN INCHES
TOLERANCES:
FRACTIONAL±
ANGULAR: MACH± BEND ±
TWO PLACE DECIMAL ±0.01
THREE PLACE DECIMAL ±0.005

INTERPRET GEOMETRIC TOLERANCING PER:

MATERIAL
6061 Aluminum

FINISH

DO NOT SCALE DRAWING

	NAME	DATE
DRAWN		
CHECKED		
ENG APPR.		
MFG APPR.		
Q.A.		

COMMENTS:

NEXT ASSY | USED ON

APPLICATION

PROPRIETARY AND CONFIDENTIAL

TITLE:
DisplacerStructureTop-1a

SIZE
A

DWG. NO.
Assem-1a

REV

SCALE: 1:2
WEIGHT:
SHEET 9 OF 14

Note: Pieces joined with JB Weld

ITEM NO.	PART NUMBER	QTY.
1	DisplacerCylinder-1a	1
2	DisplacerStructureBot-1a	1
3	DisplacerStructureTop-1a	1
4	9634K31	2

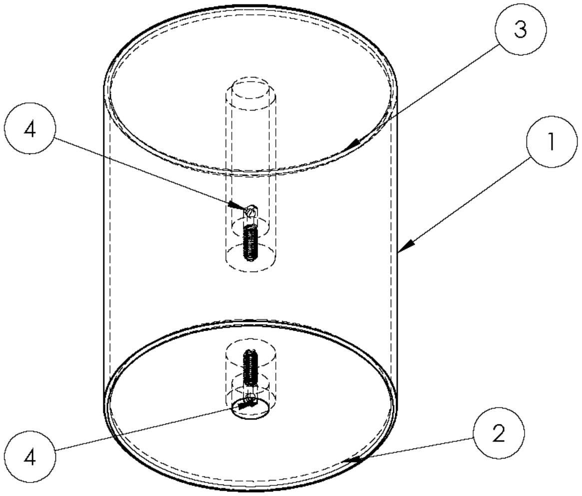

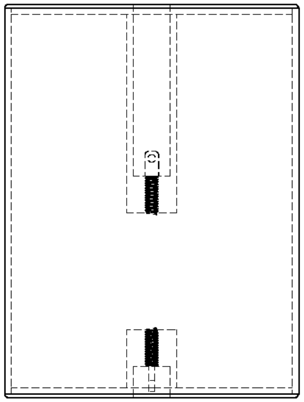

PROPRIETARY AND CONFIDENTIAL

THE INFORMATION CONTAINED IN THIS DRAWING IS THE SOLE PROPERTY OF <INSERT COMPANY NAME HERE>. ANY REPRODUCTION IN PART OR AS A WHOLE WITHOUT THE WRITTEN PERMISSION OF <INSERT COMPANY NAME HERE> IS PROHIBITED.

NEXT ASSY
USED ON
APPLICATION

UNLESS OTHERWISE SPECIFIED:
DIMENSIONS ARE IN INCHES
TOLERANCES:
FRACTIONAL±
ANGULAR: MACH± BEND ±
TWO PLACE DECIMAL ±
THREE PLACE DECIMAL ±
INTERPRET GEOMETRIC TOLERANCING PER:
MATERIAL
Aluminum
FINISH
DO NOT SCALE DRAWING

	NAME	DATE
DRAWN		
CHECKED		
ENG APPR.		
MFG APPR.		
Q.A.		

COMMENTS:

TITLE:
Displacer Assembly

SIZE **A**
DWG. NO. Assem-1a
REV
SCALE: 1:2
WEIGHT:
SHEET 10 OF 14

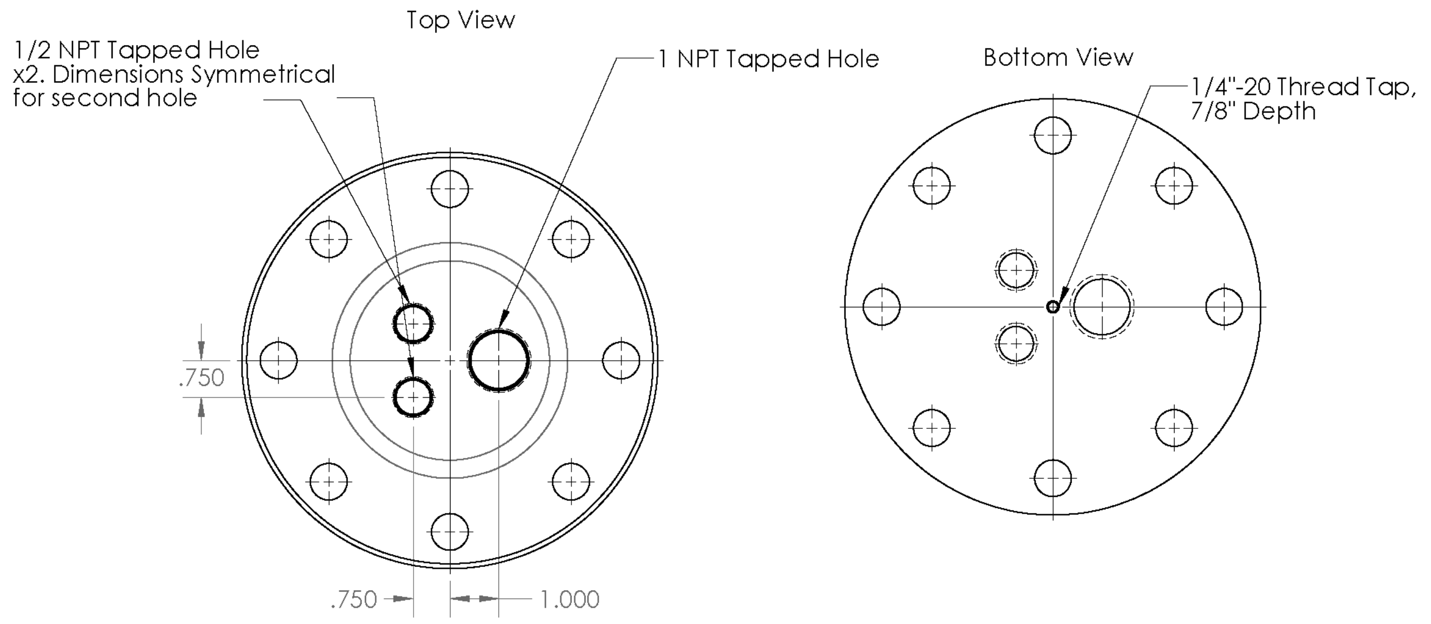

ITEM NO.	PART NUMBER	DESCRIPTION	QTY.
1	pipefittingsdirect.com SKU: KFBL3.5	3 ½ inch class 150 carbon steel blind cap flange	1

PROPRIETARY AND CONFIDENTIAL

NEXT ASSY
USED ON
APPLICATION

UNLESS OTHERWISE SPECIFIED:
DIMENSIONS ARE IN INCHES
TOLERANCES:
FRACTIONAL±
ANGULAR: MACH± BEND ±
TWO PLACE DECIMAL ±.01
THREE PLACE DECIMAL ±.005
INTERPRET GEOMETRIC
TOLERANCING PER:
MATERIAL
FINISH
DO NOT SCALE DRAWING

	NAME	DATE
DRAWN		
CHECKED		
ENG APPR.		
MFG APPR.		
Q.A.		

COMMENTS:

TITLE:

SIZE **A**
DWG. NO. Assem-1a
REV
SCALE: 1:4
WEIGHT:
SHEET 11 OF 1

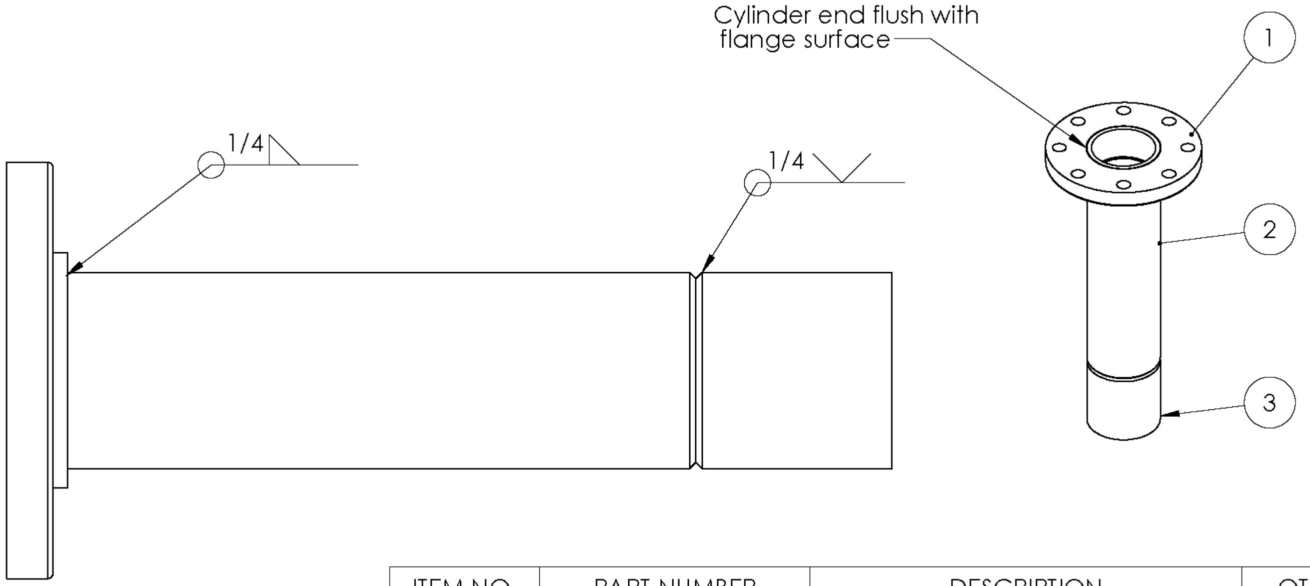

ITEM NO.	PART NUMBER	DESCRIPTION	QTY.
1	pipefittingsdirect.com SKU: KFSO3.5	3 ½ inch Slip On Class 150 Carbon Steel Flange	1
2	Cylinder-1a		1
3	EndPlug-1a		1

PROPRIETARY AND CONFIDENTIAL

THE INFORMATION CONTAINED IN THIS DRAWING IS THE SOLE PROPERTY OF <INSERT COMPANY NAME HERE>. ANY REPRODUCTION IN PART OR AS A WHOLE WITHOUT THE WRITTEN PERMISSION OF <INSERT COMPANY NAME HERE> IS PROHIBITED.

NEXT ASSY | USED ON

APPLICATION

UNLESS OTHERWISE SPECIFIED:

DIMENSIONS ARE IN INCHES
TOLERANCES:
FRACTIONAL±
ANGULAR: MACH± BEND ±
TWO PLACE DECIMAL ±
THREE PLACE DECIMAL ±

INTERPRET GEOMETRIC TOLERANCING PER:

MATERIAL

FINISH

DO NOT SCALE DRAWING

	NAME	DATE
DRAWN		
CHECKED		
ENG APPR.		
MFG APPR.		
Q.A.		

COMMENTS:

TITLE:

Weldment Cylinder Assembly

SIZE
A

DWG. NO.
Assem-1a

REV

SCALE: 1:8 WEIGHT: SHEET 12 OF 1

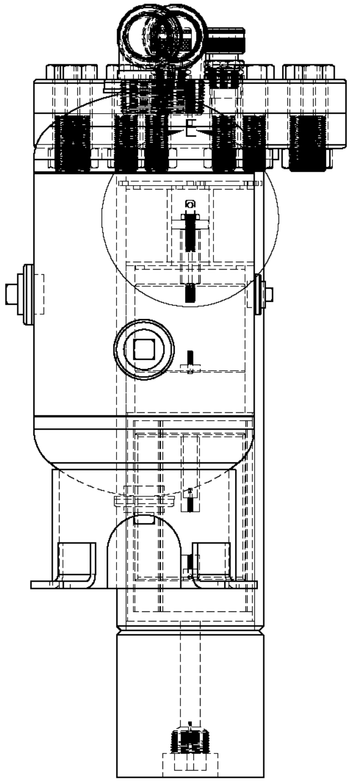

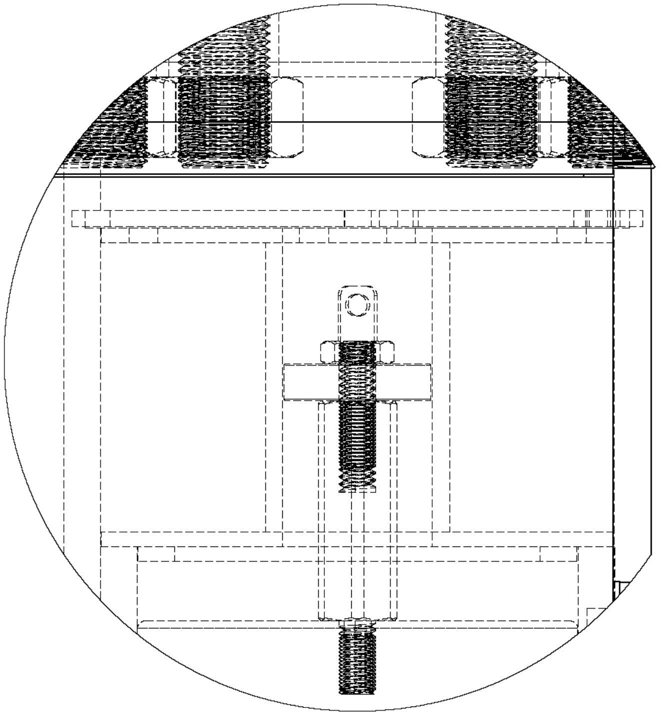

DETAIL E
SCALE 1 : 1

PROPRIETARY AND CONFIDENTIAL

THE INFORMATION CONTAINED IN THIS DRAWING IS THE SOLE PROPERTY OF <INSERT COMPANY NAME HERE>. ANY REPRODUCTION IN PART OR AS A WHOLE WITHOUT THE WRITTEN PERMISSION OF <INSERT COMPANY NAME HERE> IS PROHIBITED.

NEXT ASSY
USED ON
APPLICATION

UNLESS OTHERWISE SPECIFIED:
DIMENSIONS ARE IN INCHES
TOLERANCES:
FRACTIONAL±
ANGULAR: MACH± BEND ±
TWO PLACE DECIMAL ±
THREE PLACE DECIMAL ±
INTERPRET GEOMETRIC TOLERANCING PER:
MATERIAL
FINISH
DO NOT SCALE DRAWING

	NAME	DATE
DRAWN		
CHECKED		
ENG APPR.		
MFG APPR.		
Q.A.		

COMMENTS:

TITLE:
For better view of Standoff-Magnet-Spring Stud Assy.
See first sheet for part names

SIZE
A
DWG. NO.
Assem-1a
REV

SCALE: 1:8
WEIGHT:
SHEET 13 OF 1

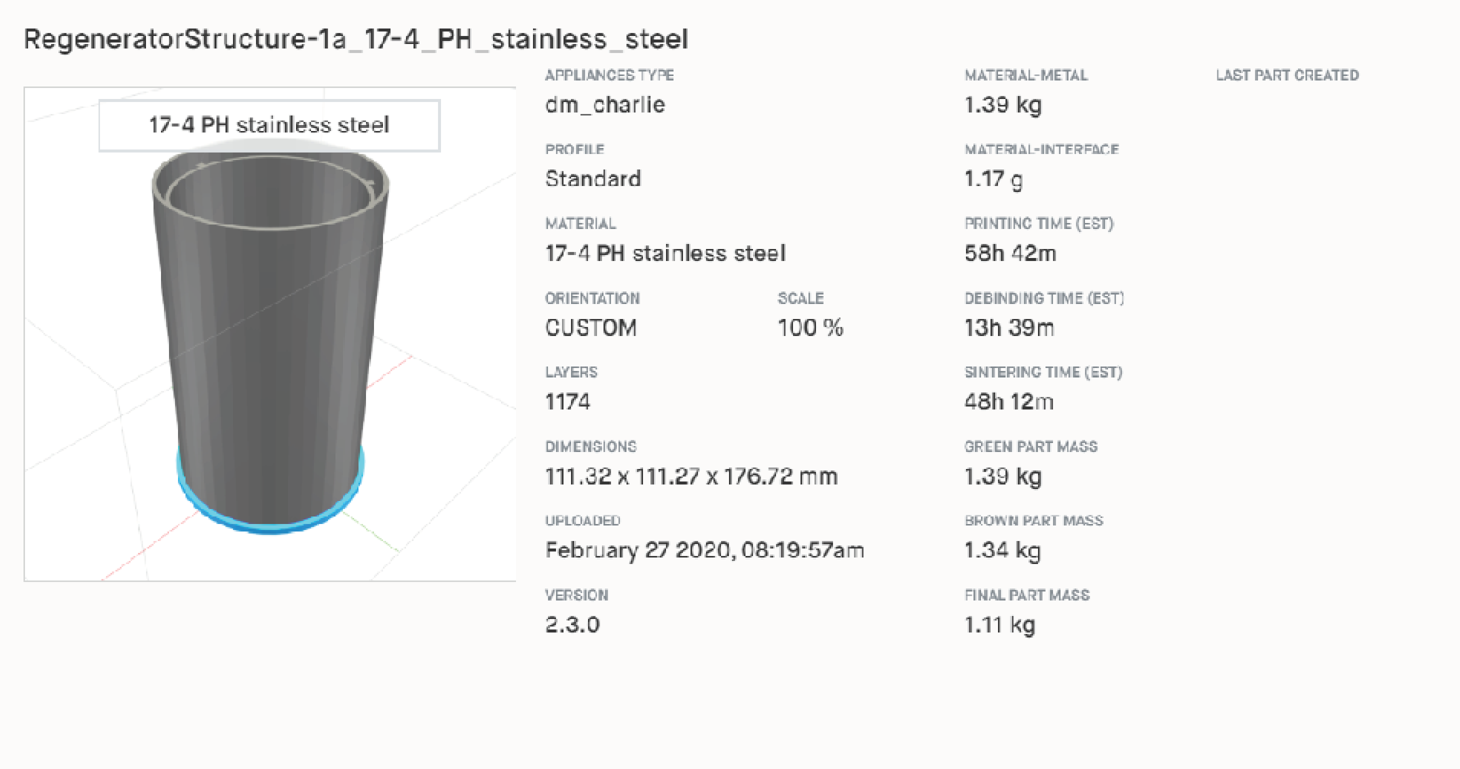

RegeneratorStructure-1a_17-4_PH_stainless_steel

APPLIANCES TYPE
dm_charlie

PROFILE
Standard

MATERIAL
17-4 PH stainless steel

ORIENTATION
CUSTOM

SCALE
100 %

LAYERS
1174

DIMENSIONS
111.32 x 111.27 x 176.72 mm

UPLOADED
February 27 2020, 08:19:57am

VERSION
2.3.0

MATERIAL-METAL
1.39 kg

MATERIAL-INTERFACE
1.17 g

PRINTING TIME (EST)
58h 42m

DEBINDING TIME (EST)
13h 39m

SINTERING TIME (EST)
48h 12m

GREEN PART MASS
1.39 kg

BROWN PART MASS
1.34 kg

FINAL PART MASS
1.11 kg

LAST PART CREATED

PROPRIETARY AND CONFIDENTIAL

THE INFORMATION CONTAINED IN THIS DRAWING IS THE SOLE PROPERTY OF <INSERT COMPANY NAME HERE>. ANY REPRODUCTION IN PART OR AS A WHOLE WITHOUT THE WRITTEN PERMISSION OF <INSERT COMPANY NAME HERE> IS PROHIBITED.

NEXT ASSY
USED ON
APPLICATION

UNLESS OTHERWISE SPECIFIED:
DIMENSIONS ARE IN INCHES
TOLERANCES:
FRACTIONAL±
ANGULAR: MACH± BEND ±
TWO PLACE DECIMAL ±
THREE PLACE DECIMAL ±

INTERPRET GEOMETRIC TOLERANCING PER:
MATERIAL
FINISH
DO NOT SCALE DRAWING

	NAME	DATE
DRAWN		
CHECKED		
ENG APPR.		
MFG APPR.		
Q.A.		

COMMENTS:

TITLE:
3D Printed Regenerator Housing

Credit to Duke Bluesmith

SIZE
A
DWG. NO.
Assem-1a
REV

SCALE: 2:1
WEIGHT:
SHEET 14 OF 1

5.6 Appendix F: Process Failure Modes and Effects Analysis

Severity Scale

Adapt as appropriate

Effect	Criteria: Severity of Effect	Ranking
Hazardous - Without Warning	May expose client to loss, harm or major disruption - failure will occur **without** warning	10
Hazardous - With Warning	May expose client to loss, harm or major disruption - failure will occur **with** warning	9
Very High	Major disruption of service involving client interaction, resulting in either associate re-work or inconvenience to client	8
High	Minor disruption of service involving client interaction and resulting in either associate re-work or inconvenience to clients	7
Moderate	Major disruption of service not involving client interaction and resulting in either associate re-work or inconvenience to clients	6
Low	Minor disruption of service not involving client interaction and resulting in either associate re-work or inconvenience to clients	5
Very Low	Minor disruption of service involving client interaction that does not result in either associate re-work or inconvenience to clients	4
Minor	Minor disruption of service not involving client interaction and does not result in either associate re-work or inconvenience to clients	3
Very Minor	No disruption of service noticed by the client in any capacity and does not result in either associate re-work or inconvenience to clients	2
None	No Effect	1

Occurrence Scale

Probability of Failure	Time Period	Per Item Failure Rates	Ranking
Very High: Failure is almost inevitable	More than once per day	>= 1 in 2	10
	Once every 3-4 days	1 in 3	9
High: Generally associated with processes similar to previous processes that have often failed	Once every week	1 in 8	8
	Once every month	1in 20	7
Moderate: Generally associated with processes similar to previous processes which have experienced occasional failures, but not in major proportions	Once every 3 months	1 in 80	6
	Once every 6 months	1 in 400	5
	Once a year	1 in 800	4
Low: Isolated failures associated with similar processes	Once every 1 - 3 years	1 in 1,500	3
Very Low: Only isolated failures associated with almost identical processes	Once every 3 - 6 years	1 in 3,000	2
Remote: Failure is unlikely. No failures associated with almost identical processes	Once Every 7+ Years	1 in 6000	1

Detection Scale

Detection	Criteria: Likelihood the existence of a defect will be detected by process controls before next or subsequent process, -OR- before exposure to a client	Ranking
Almost Impossible	No known controls available to detect failure mode	10
Very Remote	Very remote likelihood current controls will detect failure mode	9
Remote	Remote likelihood current controls will detect failure mode	8
Very Low	Very low likelihood current controls will detect failure mode	7
Low	Low likelihood current controls will detect failure mode	6
Moderate	Moderate likelihood current controls will detect failure mode	5
Moderately High	Moderately high likelihood current controls will detect failure mode	4
High	High likelihood current controls will detect failure mode	3
Very High	Very high likelihood current controls will detect failure mode	2
Almost Certain	Current controls almost certain to detect the failure mode. Reliable detection controls are known with similar processes.	1

FMEA

Process/Product Name: Part Machining/Stirling Engine

Responsible:

Prepared By: Christopher Orrico

FMEA Date (Orig.): 29-Mar

Process Step/Input	Potential Failure Mode	Potential Failure Effects	SEVERITY (1 - 10)	Potential Causes	OCCURRENCE (1 - 10)	Current Controls	DETECTION (1 - 10)	RPN	Action Recommended
What is the process step, change or feature under investigation?	In what ways could the step, change or feature go wrong?	What is the impact on the customer if this failure is not prevented or corrected?		What causes the step, change or feature to go wrong? (how could it occur?)		What controls exist that either prevent or detect the failure?			What are the recommended actions for reducing the occurrence of the cause or improving detection?
Displacer Part Manufacture	Walls too thin to support step/spring stud recess assembly, warping the displacer walls upon assembly	Displacer could jam in cylinder upon operation	8	Non-delicate assembly, screw torquing	5	Careful assembly	4	160	Replace purchased springs with custom springs of perfect length, removing need for large recesses.
Engine Cylinder Wall Manufacture	Inconsistencies between nominal ID of cylinder and measured OD of regenerator housing, sleeve bearing	Inability to assemble engine	8	Manufacturer tolerances of steel pipe/sleeve bearing too high; warping during 3D printing process of housing	9	See Action Recommended	2	144	Manufacture Regenerator housing first, measure real OD of housing, bearing. Bore cylinder to fit accordingly
Regenerator Housing	Manufacture produces unexpected or inconsistent ID/OD	Inability to assemble; Piston Jamming	8	Warping during 3D printing process	5	Account for documented warping effects in model	2	80	3D print the housing first, measure real dimensions to bore cylinder/machine displacer. Consider using different 3D printing method or casting the Regenerator Housing.

FMEA

Process/Product Name: Engine Assembly/Stirling Engine

Responsible:

Prepared By: Christopher Orrico

FMEA Date (Orig.): 29-Mar

Process Step/Input	Potential Failure Mode	Potential Failure Effects	SEVERITY (1 - 10)	Potential Causes	OCCURRENCE (1 - 10)	Current Controls	DETECTION (1 - 10)	RPN	Action Recommended
What is the process step, change or feature under investigation?	In what ways could the step, change or feature go wrong?	What is the impact on the customer if this failure is not prevented or corrected?		What causes the step, change or feature to go wrong? (how could it occur?)		What controls exist that either prevent or detect the failure?			What are the recommended actions for reducing the occurrence of the cause or improving detection?
Spring - Stud connection/insertion	Too difficult to practically assemble Piston-Displacer-Spring assembly.	Inability to assemble engine	8	Not enough space to screw in spring studs	10	N/a	1	80	Eliminate spring recesses by purchasing custom springs; preassemble spring mass train outside of engine
Regenerator Housing - Sleeve Bearing - Generator Housing	Stack is taller than designed	Inability to insert holding snap ring	7	Sleeve bearing/regenerator housing/generator housing longer than expected,	5	N/a	2	70	Machine stack components before machining cylinder groove, ensuring proper location
Housing/Bearing Stack Assembly	Stack is shorter than designed	Snap ring does not hold components in place, resulting in operation vibrations	4	Sleeve bearing/regenerator housing/generator housing shorter than expected,	5	N/a	4	80	Machine stack components before machining cylinder groove, ensuring proper location
Piston/Displacer/Spring train	Piston and displacer sit in incorrect rest positions	Collision of the piston/displacer with stack components	7	Piston/Displacer too light or heavy, springs do not match manufacturer specified k values	5	Hang stack outside of engine and measure positions to confirm is correct	7	245	No extra actions in prototype phase, consider further action for mass production
Piston - Sleeve Bearing Fit	Piston slides with too much friction	Reduced engine performance	4	Poor tolerancing during machining	3	Measure fit tolerances off of real ID of sleeve bearing	8	96	Seek machining form high precision machine shop; Measure interfacial friction prior to assembly
Displacer Assembly	Pieces do not fit orthoganolly with one another	Displacer jams during operation	8	Current design does not result in good part joint	5	Assemble with clamps that ensure orthoganol fit	8	320	Redesign displacer to have thicker walls, longer lip at joint to promote fit accuracy
Housing/Bearing Stack Assembly	Regnerator housing cannot support axial stress of stack assembly	Buckling of regenerator housing	8	3D printing part strength weaker than material properties of metal	7	FEA	5	280	Redesign regenerator housing to have thicker walls
Cylinder Wall/End Cap/Flange Weldment	Welding warps cylinder walls	Inability to assemble housing/bearing stack	8	Heat of welding	1	Careful welding	1	8	Thicker cylinder walls, different sealing process

FMEA

Process/Product Name: Use-Case/Stirling Engine
Responsible:
Prepared By: Sam Osheroff
FMEA Date (Orig.): 29-Mar

Process Step/Input	Potential Failure Mode	Potential Failure Effects	SEVERITY (1 - 10)	Potential Causes	OCCURRENCE (1 - 10)	Current Controls	DETECTION (1 - 10)	RPN	Action Recommended
What is the process step, change or feature under investigation?	In what ways could the step, change or feature go wrong?	What is the impact on the customer if this failure is not prevented or corrected?		What causes the step, change or feature to go wrong? (how could it occur?)		What controls exist that either prevent or detect the failure?			What are the recommended actions for reducing the occurrence of the cause or improving detection?
Threaded Pipe Fittings	Wire feedthrough or teflon tape does not adequately maintain the internal pressure	Engine does not operate at desired pressure	5	Pipe fitting holes aren't adequately machined. As-ordered parts are incompatible with the wires being used	3	Active bounce space pressure measurement.	1	15	Machine and thread holes in a test piece for fitting before machining on engine body; contact manufacturer or switch out wires; replace NPT fitting with CGA fittings
Pipe fittings	Abrupt fitting failure causes pipe fittings to forcibly eject from engine body	Danger to experimenters and setup from fittings moving at high velocity	9	Pipe fitting holes not adequately machined, pipe fittings not adequately inserted	2	Proper machining practices, acrylic shield present during testing	3	54	Take special care when machining and testing these fittings
Engine body	Engine body deforms under operation/placement	Components become skewed, affecting performance; in extreme case, engine body is unusable	5	Hoop or longitudinal stress due to engine operation, pipe movement, internal pressurization exceeds yield stress	1	Failure may be detected visually; high factor of safety of hoop stress in pipe wall makes failure unlikely	1	5	Alter geometry to increase component strength
Regenerator housing	Regenerator housing experiences thermal warping or melting	Fluid is not adequately moved, heat passage slows, and engine sllows	3	Thermal stress from repeated cycling of regenerator through hot end causes 3D printed regenerator component to deform	2	Parts of engine would need to be disassembled to observe failure	4	24	Implement alternative printing materials

FMEA

Process/Product Name: Testing/Stirling Engine

Prepared By: Sam Osheroff

Responsible:

FMEA Date (Orig.): 29-Ma

Process Step/Input	Potential Failure Mode	Potential Failure Effects	SEVERITY (1 - 10)	Potential Causes	OCCURRENCE (1 - 10)	Current Controls	DETECTION (1 - 10)	RPN	Action Recommended
What is the process step, change or feature under investigation?	In what ways could the step, change or feature go wrong?	What is the impact on the customer if this failure is not prevented or corrected?		What causes the step, change or feature to go wrong? (how could it occur?)		What controls exist that either prevent or detect the failure?			What are the recommended actions fo reducing the occurrence o the cause or improving detection?
Acrylic shield	Breaking due to catastrophic impact of engine failure	Potential danger to experimenters posed by pieces of acrylic or engine components moving at high speed	10	Components of pressurized engine fail individually and are forced outwards by internal pressure, generating impact forces strong enough to break the shield wall	2	Shield wall material specified to withstand impact forces	1	20	Ensure material ordered is thick enough to withstand reasonable impact forces
Acrylic shield	Movement off of or away from engine	Shield could potentially come askew, exposing experimenters to danger of pressurized parts	6	Components of pressurized engine fail individually and are forced outwards by internal pressure, knocking the wall out of place; engine vibrations cause shield to shift	3	Weight of shield and fit of shield around engine body will act to keep it in place and covering all potentially dangerous areas; engine vibration expected to only occur axually	1	18	Further weigh down shield with weights on bottom struts, resisting movement
Acrylic shield door	Providing too open of an area during operation	Experimenters are exposed to projectiles flying through the door and not being stopped by the shield wall	10	Shield door swings open due to vibrations of the full shield caused by engine vibration; shield door swings open on impact from a projectile	1	Shield door only occupies a small area on engine; shield door area will filled with wires	1	10	Carefully measure aggregate size of wire bundle to ensure that shield door size is not excessively large. Explore alternate sliding door construction
Cooling coil	Cooling coil does not adequately lower heat of cold generator side	Engine does not produce desired amount of energy, or move at desired frequency	3	Pump does not move water at high enough speed to achieve desired cooling; water is not cold enough to achieve desired cooling	7	Pipe material ordered to maximize cooling; pump ordered to move water reliably through desired distance of pipe	5	105	Have alternative pumps in case the specified pump fails to move enough water; experiment to find ideal pump orientation; use coolant liquid to supercool water

5.7 Appendix G: Bill of Materials

Item	Price/Unit	Qty	Total	Duke ME Lab Total	Details	Link
Springs						
Extension Spring (Displacer)	17.23	1	17.23	17.23	2" Long, 0.5" OD, 0.041" Wire Diameter, 1.59 lb/in, pack of 3	https://www.mcmaster.com/1920N44
Extension Spring (Displacer-Piston)	4.29	1	4.29	4.29	3" Long, 0.375" OD, 0.045" Wire Diameter, Rate 2.78 Lb/in, pack of 3	https://www.mcmaster.com/9433K73
Extension Spring (Piston)	10.12	1	10.12	10.12	2.75" Long, 0.5" OD, 0.063" Wire Diameter, 7.99 lb/in, pack of 3	https://www.mcmaster.com/9065K375
Cylinder						
Low-Carbon Steel Round Tube,	213.61	1	213.61	213.61	1/4" Wall Thickness, 4" OD, 36" Length	https://www.mcmaster.com/7767t77-7767T771
Low-Carbon Steel Disc	82.46	1	82.46	82.46	6" Long, 4" Diameter	https://www.mcmaster.com/7786t58
Oil-Resistant Compressible Buna-N Gasket	7.74	1	2.36	2.36	1/16 in thick	https://www.mcmaster.com/8516t239-8516T33
3 ½ inch Slip On Carbon Steel Flange	19.28	1	19.28	19.28	Flange, 3.5 Pipe Size	150-carbon-steel-flanges-2-2
3 ½ inch class 150 carbon steel blind cap flange	24.4	1	24.4	24.4	Cap, 3.5 Pipe Size	steel-blind-flange
Medium-Strength Grade 5 Steel Hex Head Screw	12.99	1	12.99	0	5/8"-18 Thread Size, 2-1/2" Long, Partially Threaded, pack of 10	https://www.mcmaster.com/91247a438
Medium-Strength Steel Hex Nut	8.38	1	8.38	0	Grade 5, Zinc-Plated, 5/8"-18 Thread Size, pack of 25	https://www.mcmaster.com/95462a535
316 Stainless Steel Split Lock Washer	4.39	1	4.39	0	for 5/8" Screw Size, 0.641" ID, 1.073" OD, pack of 10	https://www.mcmaster.com/92147a035
Internal Retaining Ring□	3.01	1	3.01	3.01	for 3-1/2" ID, Black-Phosphate 1060-1090 Spring Steel	https://www.mcmaster.com/99142A670
Low-Pressure Pipe Fitting	0.84	1	0.84	0.84	Steel, Solid Plug with External Square Drive, 3/4 NPT	https://www.mcmaster.com/44605k225
Displacer						
Multipurpose 6061 Aluminum, 3" Diameter Round	5.74	1	5.74	0	3" long, 1610T19	https://www.mcmaster.com/1610t19-1610T125
Multipurpose 6061 Aluminum, 3" Diameter Round	8.61	1	8.61	0	1" long, 1610T19	https://www.mcmaster.com/1610t19-1610T125
Multipurpose 6061 Aluminum Round Tube	24.39	1	24.39	24.39	6" long, 0.065" Wall Thickness, 3" OD	https://www.mcmaster.com/9056k85-9056K855
Piston						
Neodymium Magnet with Straight Unthreaded Hole	8.55	1	8.55	8.55	Thickness: 0.25 in, OD 1 in, hole diameter 0.25 in	https://www.mcmaster.com/3360K862
Oil-Embedded Bronze Sleeve Bearing	77.88	1	77.88	77.88	for 3" Shaft Diameter and 3-1/2" Housing ID, 4" Long	https://www.mcmaster.com/6391k471
AWG 22 Enameled Copper Wire (507' (152m))	16.41	1	16.41	16.41	Will need ~6m per coil housing	https://amzn.to/2xaJyaN
Male-Female Threaded Hex Standoff	4.97	1	4.97	4.97	Aluminum, 1/2" Hex Size, 1-1/2" Long, 1/4"-20 Thread Size	https://www.mcmaster.com/93505a199
Aluminum Thin Hex Nut	9.66	1	9.66	9.66	1/4"-20 Thread Size	https://www.mcmaster.com/91947a110
Extension Spring Stud Anchor	3.16	3	9.48	9.48	6-40 Thread Size	https://www.mcmaster.com/9634k31
Extension Spring Stud Anchor	3.4	2	6.8	6.8	1/4"-20 Thread Size, 0.15" Hole Diameter	https://www.mcmaster.com/9634k23
Low-Carbon Steel Disc	26.52	1	26.52	0	3" Long, 3" Diameter	https://www.mcmaster.com/7786t36
Bounce Space						
Low-Pressure Pipe Fitting Elbow	6.4	2	12.8	12.8	Iron, 90 Degree Elbow Adapter, 1 NPT Female x Male	https://www.mcmaster.com/44605k136
Standard-Wall Steel Pipe Nipple	6.82	1	6.82	6.82	Threaded on Both Ends, 1 NPT, 8" Long	https://www.mcmaster.com/44615k526
Vertical ASME-Code Compressed Air Storage Tank	296.36	1	296.36	0	Powder Coated Steel, 1 Gallon Capacity	https://www.mcmaster.com/1584k1
				0		
Regenerator				0		
Copper Gauze	51.33	1	51.33	51.33	5" x 100ft	https://www.mcmaster.com/6361t12
Regenerator Housing	218.14	1	218.14	218.14	Metal 3D printing, 17 4 stainless	https://www.bluesmith.oit.duke.edu
Heating/Cooling						
1/4" OD Copper Coil	19.97	1	19.97	19.97	1/4" OD x 20 ft	Copper-Refrigeration-Coil-Tubing-1-4-R-20RE/203654224
SEAFLO 21-Series Diaphragm Water Pump	29.99	1	29.99	0	1.2 gpm, 3/8" hose leads	https://www.seaflo.us/product/21-series-diaphragm-water-pumps/
Solder-Joint Fitting	4.85	2	9.7	9.7	1/4" pipe OD Female Socket-connect Tube x 1/4" Female NPT	https://www.mcmaster.com/5520K174
Barbed NPT/hose fitting	1.98	2	3.96	3.96	3/8" Hose ID, 1/4" male threaded pipe	https://www.mcmaster.com/5350K36
Hose clamps				0	for 3/8" ID hose	
Hose	9.2	1	9.2	9.2	3/8" OD	https://www.mcmaster.com/5233K65
Power cable to pass through strain relief	15.6	1	15.6	15.6	3ft (qty 3),Item # 24C155, Continuous Flexing Power Cable, 8 AWG	https://bit.ly/2Y6INdZ
Liquidtight Straight Strain Relief Cord Grip	9.29	1	9.29	9.29	0.15 to 0.25" 1/2 NPT, 1-5/16" OAL, Steel	https://www.mscdirect.com/product/details/04499141
Band Heater	57.52	1	57.52	57.52	900°F, 120VAC, Watts 400, Inside Dia. 4", Width 1"	https://www.grainger.com/product/TEMPCO-Band-Heater-2VYK2
Insulation	20.98	1	20.98	20.98		https://thd.co/2zxweOG
		Totals	1364.03	971.05		
	Cost/Unit	**Qty**	**Price**	**ME Lab Total**		
Testing						
80/20 1010 T-channel	$48.06	1	$48.06	$48.06	1 x 99", 1 x 93" (max 102" per piece)	https://8020.net/1010.html
4 hole adjustable panel hinge	$7.30	1	$7.30	$7.30		https://8020.net/2081.html
Inside brackets	$2.90	16	$46.40	$46.40		https://8020.net/4119.html
Cap Screws	$0.23	32	$7.36	$7.36	1/4-20 x .500" Button Head Socket Cap Screw (BHSCS)	https://8020.net/3061.html
T-nuts	$0.21	32	$6.72	$6.72	1/4-20 Slide-in Economy T-Nut - Centered Thread	https://8020.net/3382.html
Polycarbonate sheet	$41.14	2	$82.28	$82.28	1/8" thick, 24x48"	https://www.mcmaster.com/catalog/126/3815
		Total:	$198.12	$198.12		

5.8 Appendix H: Assembly Procedure

1. 3D print the Regenerator Housing.
   The plan of this team was to 3D print the housing using 17 4 PH stainless steel printed on a Desktop Metal Studio System™ printer. We recommend prototyping this component in metal due to its need to have relatively high thermal conductivity and withstand the temperatures of the piston cylinder hot end without significant warping.
2. Critical-to-function dimension measurement for piston cylinder components to 3 significant figures.
   a. Regenerator Housing:
      i. Length
      ii. ID
      iii. OD
   b. Sleeve Bearing
      i. Length
      ii. ID
      iii. OD
   c. Steel Pipe (For piston cylinder).
      i. ID
3. 3D print the Generator Housing.
   This step can be done using any thermoplastic (PLA, ABS, etc) through basic FDM printing (such as on an Ultimaker S3). Measure the OD and ID of the final product and verify that it meets the tolerances of the technical drawings.
4. Machine the Steel Pipe for use as the Piston Cylinder.
   a. Calculate amount of bore needed along the length of the steel pipe needed to fit components of the housing bearing stack (from top to bottom: Generator Housing, Sleeve Bearing, Regenerator Housing).
   b. For the measured length of each component (see step 2), bore the steel pipe to the required tolerance fit specified in the technical drawings. Note: In the case that a top component has a smaller outer diameter than one of the components below it in the stack, machine the outer diameters of the stack components below it to be less than the smallest component. For example, if the Generator Housing has a smaller outer diameter than the Sleeve Bearing, reprint the Generator Housing to be slightly wider than the sleeve bearing.
   c. Given the measured stack length, machine groove for snap ring.
5. Wind the Generator Coil around the Generator Housing.
   AWG #22 wire was chosen as the wiring for the generator considering a trade-off between maximizing number of turns (smaller diameter) and lower resistance (higher diameter). This step can be done manually using a power drill or semi-automatically on a drill press or mill. This winding method describes a procedure that creates 4 terminals, allowing the user to vary the amount of wire coils connected to the dummy resistor circuit by half, altering the effective electromagnetic damping of the engine system. Note that additional steps would be necessary to set the RPM of any CNC equipment that is used to manufacture the generator coil on a mill, so this should be considered when deciding

what equipment to use. These instructions will be explained for a power drill. Refer to figure 16 as a supplement to the following steps. The blue wire is wire A and the orange wire is wire B.

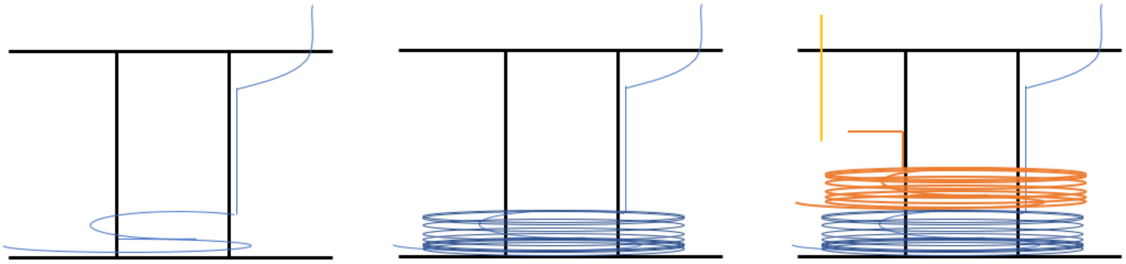

Figure 16: Schematic of Spool Wiring

a. Setup of spool:
    i. Place an approx. 1" diameter rubber piece in the generator housing's center hole. This piece should be sturdy enough to drive the rotation of the housing but soft enough such that a dowel rod can be inserted with ease.
    ii. Insert dowel rod (most likely wooden), that is small enough such that it can be grasped with ease by a power drill. Make sure that when turning, the housing does not wobble too much.
    iii. Make markings 2 cm & 4 cm off the bottom of the housing's space where the wire will be wound.
b. Winding Wire A:
    i. From the purchased spool of wire, pull >1' of wire. Then wrap the bottom of that wire (non-loose end) a few times around the bottom of the housing. Thread the loose end of the wire through the holes at the top of the housing. Tape down the rest along the vertical height of the spool.
    ii. Once a few turns are secured, turn on the power drill slowly and start winding additional turns of wire. With one hand grab the spool, with the other adjust the power drill's turning speed.
    iii. The sequence of filling the wire is first to fill the distance from 0-2cm mark with a 'layer' of wire. Then build as many layers as possible in the radial direction up until the radial distance at which the holes from which the wire was thread.
    iv. Once the 0-2 cm space was filled radially and vertically, cut the wire with enough extra wire to solder a connection to a wire leaving the piston cylinder.
c. Winding Wire B:
    i. From the purchased spool of wire, pull approximately 6" of wire. Then wrap the bottom of that wire (non-loose end) a few times around the 1" housing diameter above Wire A, then tape the loose end along the vertical height of the spool.
    ii. Continue winding similar to as in Wire A from 2-4cm.

        - iii. Cut the wire. Thread a separate piece of wire from the top of engine down to Generator Housing to complete circuit
    - d. When Wire A & B want to be used: connect their loose ends by tying the ends and using electrical tape. Then connect the other loose end of Wire B to the external wire that was last threaded into the housing. If only Wire A wants to be used, connect external wire that was last threaded to Wire A' loose thread.
6. Machine the End Plug and accompanying End Plug Pipe Fitting as specified in the technical drawings.
7. Machine the Piston.
    - a. On a lathe, machine the Piston to meet the tolerances specified by the technical drawings using the measured ID of the Sleeve Bearing.
    - b. Tap and thread holes for Spring Studs.
8. Machine the Displacer
    - a. On a lathe, machine the Displacer components (Displacer Cylinder, Displacer Structure Top, Displacer Structure Bottom) to meet the tolerances specified by the technical drawings using the measured ID of the Regenerator Housing.
    - b. Tap and thread holes for Spring Studs.
    - c. Using JB Weld on the internal connections between the Displacer components, assemble the Displacer ensuring a 90-degree angle between all components.
9. Hang the Piston-Displacer-Spring assembly to ensure proper resting positions (See section 3.2.3). If they hang in the incorrect positions, consider the following steps.
    - a. Check masses of displacer and piston. If incorrect, make changes accordingly and rehang.
    - b. If masses are correct and positions are still incorrect, contact spring manufacturer and reorder springs to correct k values.
10. Machine spring stud thread and pipe fitting threads into Blind Cap Flange.
11. Weld the Slip on Pipe Flange and Bottom End Cap to the Piston Cylinder (see welding diagram)
12. Assemble the Regenerator Housing, Sleeve Bearing, and Generator Housing stack and insert the Snap Ring.
13. Insert Piston-Displacer-Spring Assembly
    - a. Remove the Piston-Displacer-Spring assembly from the hanging rig and insert it into the Piston Cylinder Assembly with the End Plug removed from the End Cap.
    - b. Grasp the bottom spring through the threaded End Plug hole and attach it to the Spring Stud in the End Plug.
    - c. Wrap teflon tape around the End Plug threads and insert back into End Cap, torque lightly to ensure seal.
14. Place and secure Blind Cap Flange
    - a. Place the Gasket in its rough position on the Slip On Flange
    - b. Run wires from the Linear Generator through the wire Strain Relief pipe fitting holes in the Cap Flange.
    - c. Connect the top Spring connected to the Piston to the Spring Stud on the Cap Flange, being careful not to overextend the Piston Spring.
    - d. Align the holes of the Slip On Flange, Cap Flange, and Gasket.

    e. Insert the eight Bolts, Nuts, and Lock Washers into the Flange holes and torque based on Buna-N Gasket literature recommendations.

15. Connect Pipe Fittings

    All pipe thread should be connected using airtight Teflon tape.

    a. Pull wires through Strain Reliefs and insert Strain Reliefs into respective pipe threads on the Cap Flange. Torque until airtight.
    b. Connect the Pipe Elbows to the Bounce Space and Cap Flange Thread positions. Connect the Pipe Elbows via the Pipe Nipple.
    c. Check all connections to ensure a good seal.

5.9 Appendix I: Experimental Assembly Construction

1. Test shield construction
    a. Cut the 80/20 T-Channel to the following lengths: 4x10.5”, 2 x 23.5”, 2x12.5”, 4x19.5”
    b. Cut the ⅛” polycarbonate to the following dimensions:

        4 panes of 19.5” x 12.5”

        1 pane of 12.5” x 12.5”

    c. Cut a passthrough door of 3” x 4” out of one of the 19.5” x 12.5” panes.
    d. Cut a hole in the top of the 12.5” x 12.5” pane for bounce space attachment
    e. Drill holes ½” from the edges of each side of the polycarbonate panes for attachment to the 80/20 structure, as well as holes for the hinge connected to the passthrough door.
    f. Assemble the shield as shown in the drawing:

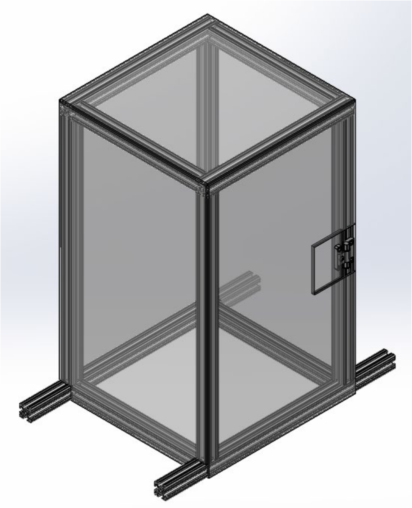

Figure 17: Test Shield

        i. Assemble the 80/20 framework by attaching joints with the Inside brackets (part 4119), cap screws, and T-nuts.
        ii. Attach the 4 hole adjustable panel hinge to the 80/20 framework and passthrough door with T-nuts and cap screws
        iii. Attach the side and top panels to the 80/20 framework with remaining T-nuts and cap screws
2. Heating coil setup
    a. Wrap and secure the TEMPCO band heater around the part of the engine directly above the end plug by screwing down the provided attachment bolt.
    b. Attach wires to band heater terminals for power and ground.
3. Cooling coil setup
    a. Cut the ¼” OD copper coil to a length of 14’.

   b. Follow proper procedures to solder-connect the two solder-joint fittings (McMaster part 5520K174) to the ends of the cut copper coil.
   c. Wrap the copper coil around the engine assembly, starting at an area 4” above the top of the band heater.
   d. Cut the 3/8” ID hose to one length of 3’, one length of 3’, and one length of 1’.
   e. Attach the 2’ hose to the free end of one of the solder-connect fittings, and the 3’ hose to the other solder-connect fitting.
   f. Attach the free end of the 2’ hose to one of the barbed pump connections on the SEAFLO 21-series diaphragm water pump.
   g. Attach the 1’ hose to the other water pump barbed connection.
   h. Feed the 1’ hose and the 3’ hose to a large reservoir of cool water.
   i. Connect the pump to 12VDC power and ensure that the pipe attains and maintains flow.
   j. Disconnect the hose from the barbed pump connection for remaining test shield setup.

4. Instrumentation
   Attach thermocouples to the engine body in the following locations:
   a. Top of heating coil area
   b. Bottom of cooling coil area
   c. Top of cooling coil area
5. Test shield setup
   a. Open passthrough door.
   b. Place test shield over engine assembly.
   c. Feed cooling coil tube, heating coil wires, generator wires, and thermocouple wires through passthrough door
6. Pressure connections
   Secure bounce space connection pipe to pressure inlet on top of engine
7. Electrical connections
   a. Connect cooling coil and heating coil thermocouples to DAQ input pins.
   b. Connect heating coil ground wire to ground.
   c. Connect heating coil power wire to control transistor
      i. Connect transistor base pin to DAQ output
      ii. Connect transistor emitter pin to heating coil power wire
      iii. Connect transistor collector pin to 120VAC power
   d. Connect regenerator wires to dummy resistor
      i. Connect two 1 Ω resistors in parallel
      ii. Connect regenerator wires to either end of parallel resistor network
      iii. Connect probe wires for measuring voltage to ends of parallel resistor network and to DAQ board.
   e. Structure LabVIEW VI to establish PID control of output power to heating coil via transistor based on heating coil thermocouple input, as well as collecting data on hot side temperature, cold side temperatures, and voltage across the resistor network.
8. Cooling coil reattachment

a. Reattach 2’ hose to barbed pump connection
b. Feed free hose ends to cool water reservoir
c. Connect pump to 12VDC power

5.10 Appendix J: Hand Calculations

5.10.1 Linear generator analysis

The number of turns *N* of wire with gauge *g* that can fit in a slot with rectangular cross-section of dimensions *w* and *h* can be estimated as follows:

$$N = \frac{w * h * k}{g^2} \quad \text{Eq (19)}^{60}$$

Where *k* represents a “filling factor”, an estimate of how well we wind the coil. While industrial windings use *k* values above 0.9, a conservative 0.6 was used to estimate the total number of turns: 1312.

5.10.2 Heat flux calculations

To calculate the heat flux needed, the amount of energy required (Q_{needed}) to heat up the mass of helium (m) inside by $\Delta T = 200\mathrm{K}$ is estimated. $\mathrm{c_p}$ is the heat capacity of helium.

$$Q_{needed} = \mathrm{mc_p}\Delta T \quad \text{Eq (20)}$$

For our system oscillating with frequency f, and with a hot volume lateral surface A_s, the heat flux required by our system is:

$$\frac{P_{needed}}{A_s} = \frac{f * Q_{needed}}{A_s} \quad \text{Eq (21)}$$

A value of about 9.1 $\frac{W}{in^2}$ is obtained. Therefore, the TEMPCO band heater with heat flux 35 $\frac{W}{in^2}$ is sufficient for our system.

---

[60] Ather

5.11 Appendix K: Test Procedures

The following procedures should be conducted with working fluids and internal pressures in the following order: I. air, 1.01 bar; II. air, 2 bar; III. helium, 1.01 bar; IV. helium, 2 bar.

1. Connect working fluid (air or helium) to bounce space pressure inlet.
2. Feed working fluid into bounce space until test pressure is attained. If changing working fluids, open engine pressure release and pressurize with working fluid for 15 minutes.
3. Run LabVIEW VI such that the hot side reaches a temperature of 200°F.
4. Maintain the hot side at 200°F for 4 minutes, reading voltage and temperature measurements to ensure successful startup and continued function.
    a. For troubleshooting startup errors, refer to the PFMEA included in Appendix D.
5. After test run is completed, safely shut down the experimental setup.
    a. Turn off power to the heating coil and pump and wait for measured temperature in heating coil to reach room temperature.
    b. Empty excess water in cooling coil tube.
    c. Disconnect wires from DAQ board.
    d. Disconnect bounce space from engine body.
    e. Remove test shield, taking care to pass wires and tubes back through passthrough door.
    f. Inspect engine body for damage
6. Repeat testing using above sequence of working fluids and internal pressures.

5.12 Appendix L: Life Cycle Analysis Results

Table 8: Sustainable Minds estimates for construction, 1 kW Stirling Engine

	Total CO2 Equivalent Emissions (kg)	Total weighted negative social impacts (MPTS)
Manufacture of engine	540	-
Energy used in transportation of materials and production	180	-
Total	720	520 (composite value)

Table 9: Sustainable Minds estimates for operation, laundromat dryer application

	Total CO2 Equivalent Emissions avoided (kg) per year	Total weighted negative social impacts (MPTS) avoided per year through waste heat recovery
Operation of 1kW Stirling Engine for dryer application	3200	110

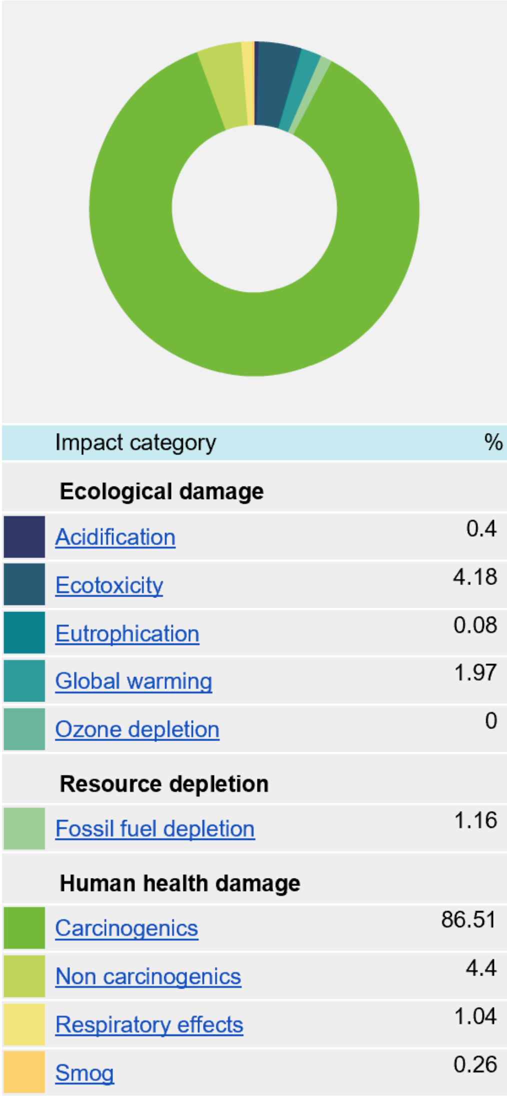

	Impact category	%
	Ecological damage	
🟦	Acidification	0.4
🟦	Ecotoxicity	4.18
🟦	Eutrophication	0.08
🟦	Global warming	1.97
🟩	Ozone depletion	0
	Resource depletion	
🟩	Fossil fuel depletion	1.16
	Human health damage	
🟩	Carcinogenics	86.51
🟩	Non carcinogenics	4.4
🟨	Respiratory effects	1.04
🟨	Smog	0.26

Figure 18: Sustainable Minds environmental impact categories for construction of a 1kW Stirling Engine by percent of overall estimated impact

6 References

Adhikari, Prakash. “Feasibility study of waste heat recovery from laundry facility : Case study: Mr Washing Man Oy.” (2017).

Association for Iron & Steel Technology. “Interactive Steel Manufacturing Process.”. Association for Iron & Steel Technology, 2020. https://www.aist.org/resources/the-msts-steel-wheel/.

Ather, S. Hussain. “Coil Winding Basics.” Sciencing, September 9, 2019. https://sciencing.com/coil-winding-basics-7480758.html.Barry Schneider, email message and phone interview with Kate White, March 3, 2020

Bawden, Tom. “Global Warming: Data Centres to Consume Three Times as Much Energy in next Decade, Experts Warn.” *Independent*, January 23, 2016. https://www.independent.co.uk/environment/global-warming-data-centres-to-consume-three-times-as-much-energy-in-next-decade-experts-warn-a6830086.html.

David Denkenberger, PhD, Serena Mau, and Chris Calwell,. “Residential Clothes Dryers: A Closer Look at Energy Efficiency Test Procedures and Savings Opportunities.” Natural Resources Defense Council. November 2011. https://www.nrdc.org/sites/default/files/ene_14060901b.pdf.

Ebrahimi, Babak, Mir Behrad Khamesee, and Farid Golnaraghi. “Eddy Current Damper Feasibility in Automobile Suspension: Modeling, Simulation and Testing.” Smart Materials and Structures 18, no. 1 (December 15, 2008): 15017. https://doi.org/10.1088/0964-1726/18/1/015017

Electric Choice. “Electricity Rates by State (Updated April 2020).” Accessed April 25, 2020. https://www.electricchoice.com/electricity-prices-by-state/.

Energy Information Administration. “U.S. Energy Information Administration - EIA - Independent Statistics and Analysis.” EIA. Accessed April 25, 2020. https://www.eia.gov/electricity/monthly/epm_table_grapher.php?t=epmt_5_6_a.

Engineering ToolBox. “Thermal Conductivity of Selected Materials and Gases.” Accessed April 5, 2020. https://www.engineeringtoolbox.com/thermal-conductivity-d_429.html.

Environmental Protection Agency. “U.S. Renewable Electricity Market.” EPA, April 9, 2019. https://www.epa.gov/greenpower/us-renewable-electricity-market.

Eriksson, Sandra. “Design of Permanent-Magnet Linear Generators with Constant-Torque-Angle Control for Wave Power.” *Energies*, vol. 12, no. 7, 5 Apr. 2019, p. 1312., doi:10.3390/en12071312.

Iceotope. “Chassis-Level Immersion Cooling”. Accessed April 9, 2020. https://www.iceotope.com/technologies/chassis-level-immersion-cooling/.

Johnson, Ilona, and William Choate. “Waste Heat Recovery: - Technology and Opportunities in U.S. Industry -,” 2008.

Karabulut, Halit. “Dynamic Analysis of a Free Piston Stirling Engine Working with Closed and Open Thermodynamic Cycles.” Renewable Energy 36, no. 6 (June 2011): 1704–9. https://doi.org/10.1016/j.renene.2010.12.006

Khodabandeh, Erfan, Mohsen Ghaderi, Abolfazl Afzalabadi, Abel Rouboa, and Amir Salarifard. “Parametric Study of Heat Transfer in an Electric Arc Furnace and Cooling System.” Applied Thermal Engineering 123 (2017): 1190–1200. https://doi.org/10.1016/j.applthermaleng.2017.05.193.

Khripach, Nanatolyevich, Ivanov, Denis, Lezhnev, Lev Yurievich, and Fedor Andreevich Shustrov. “Calculation Studies of a Free-Piston Stirling Engine.” Jr. of Industrial Pollution Control 33(2)(2017) pp 1603-1611.

Knight, Josiah. conversation with author, April 2, 2020

Marsh, Jacob. “How Hot Do Solar Panels Get? PV Temperature Explained: EnergySage.” Solar News. EnergySage, August 1, 2019. https://news.energysage.com/solar-panel-temperature-overheating/.

Martelaro, Nikolas. “Energy Use in US Steel Manufacturing,” December 4, 2016. http://large.stanford.edu/courses/2016/ph240/martelaro1/.

Monroe, Mark. “How to Reuse Waste Heat from Data Centers Intelligently.” Data Center Knowledge, May 10, 2016. https://www.datacenterknowledge.com/archives/2016/05/10/how-to-reuse-waste-heat-from-data-centers-intelligently.

Moran, M., Shapiro, H., Boettner, D. & Bailey, M. (2011). Gas Power Systems. *Fundamentals of engineering thermodynamics*. Hoboken, N.J: Wiley.

Paul, Partha, Chetan Ingale, and Bishakh Bhattacharya. “Design of a Vibration Isolation System Using Eddy Current Damper.” Proceedings of the Institution of Mechanical Engineers, Part C: Journal of Mechanical Engineering Science 228, no. 4 (May 10, 2013): 664–75. https://doi.org/10.1177/0954406213489408

Riofrio, Jose A., Khalid Al-Dakkan, Mark E. Hofacker, and Eric J. Barth. “Control-Based Design of Free-Piston Stirling Engines.” In 2008 American Control Conference. IEEE, 2008. https://doi.org/10.1109/acc.2008.4586709

Shehabi, Arman, Sarah Smith, Dale Sartor, Richard Brown, Magnus Herrlin, Jonathan Koomey, Eric Masanet, Nathaniel Horner, Inês Azevedo, and William Lintner. *United states data center energy usage report*. No. LBNL-1005775. Lawrence Berkeley National Lab.(LBNL), Berkeley, CA (United States), 2016.

Sinha-Spinks, Tracey. “The Iron and Steel Manufacturing Process.” Thermo Fisher Scientific , April 22, 2016. https://www.thermofisher.com/blog/metals/how-is-it-made-an-infographic-of-the-iron-and-steel-manufacturing-process/.

Sowale, Ayodeji, and Athanasios Kolios. “Thermodynamic Performance of Heat Exchangers in a Free Piston Stirling Engine.” Energies 11, no. 3 (February 27, 2018): 505. https://doi.org/10.3390/en11030505

Stumpf, Calynn & Hunt, Alexander & Nobes, David. (2018). Effect of Scaling Up Low Temperature Differential Stirling Engines.

Susana, Oros Teodora, et al. “Linear Generator for a Free Piston Stirling Engine.” *Journal of Electrical and Electronics Engineering*, vol. 7, no. 1, 1 Jan. 2014, pp. 111–116

US Department of Energy. “Waste Heat Recovery: -Technology and Opportunities in U.S. Industry.”. Last Modified March 2008. http://www.heatispower.org/wp-content/uploads/2011/11/waste_heat_recovery-1.pdf

Varotsis, Alkaios. “CNC Machining Is More Accessible Than You May Think.” Manufacturing.net, September 5, 2018. https://www.manufacturing.net/industry40/article/13245730/cnc-machining-is-more-accessible-than-you-may-think.

Worlds Way. “The (Many) Benefits of Outsourcing Your Manufacturing.” Worlds Way. Accessed April 25, 2020. https://worldsway.com/the-many-benefits-of-outsourcing-your-manufacturing/.

Zare, Sh., and A.R. Tavakolpour-Saleh. “Frequency-Based Design of a Free Piston Stirling Engine Using Genetic Algorithm.” Energy 109 (August 2016): 466–80. https://doi.org/10.1016/j.energy.2016.04.119